1 **Serotonin signals through postsynaptic $G\alpha_q$, Trio RhoGEF, and diacylglycerol to promote**

2 ***C. elegans* egg-laying circuit activity and behavior**

3 Pravat Dhakal, Sana I. Chaudhry, Rossana Signorelli, and Kevin M. Collins*

4 Department of Biology, University of Miami, Coral Gables, FL, United States of America

5 *To whom correspondence should be addressed. Email: *kevin.collins@miami.edu*

6 *65 pages with 7 Figures, 3 Tables and 3 Movies*

Abstract

Activated $G\alpha_q$ signals through Phospholipase-Cβ (PLCβ) and Trio, a Rho GTPase exchange factor (RhoGEF), but how these distinct effector pathways promote cellular responses to neurotransmitters like serotonin remains poorly understood. We used the egg-laying behavior circuit of *C. elegans* to determine whether PLCβ and Trio mediate serotonin and $G\alpha_q$ signaling through independent or related biochemical pathways. Our genetic rescue experiments suggest that PLCβ functions in neurons while Trio RhoGEF functions in both neurons and the postsynaptic vulval muscles. While $G\alpha_q$, PLCβ, and Trio RhoGEF mutants all fail to lay eggs in response to serotonin, optogenetic stimulation of the serotonin-releasing HSN neurons restores egg laying only in PLCβ mutants. PLCβ mutants showed vulval muscle Ca^{2+} transients while strong $G\alpha_q$ and Trio RhoGEF mutants had little or no vulval muscle Ca^{2+} activity. Treatment with phorbol 12-myristate 13-acetate (PMA) that mimics 1,2-diacylglycerol (DAG), a product of PIP_2 hydrolysis, rescued egg-laying circuit activity and behavior defects of $G\alpha_q$ signaling mutants, suggesting both Phospholipase-C and Rho signaling promote synaptic transmission and egg laying via modulation of DAG levels. DAG activates effectors including UNC-13, however we find that phorbol esters, but not serotonin, stimulate egg laying in *unc-13* and PLCβ mutants. These results support a model where serotonin signaling through $G\alpha_q$, PLCβ, and UNC-13 promote neurotransmitter release, and that serotonin also signals through $G\alpha_q$, Trio RhoGEF, and an unidentified, PMA-responsive effector to promote postsynaptic muscle excitability. Thus, the same neuromodulator serotonin can signal in distinct cells and effector pathways to coordinate activation of a motor behavior circuit.

Introduction

Neurons communicate in circuits via synaptic transmission to initiate, sustain, and terminate behaviors. During neurotransmission, both synaptic vesicles and dense-core vesicles fuse with the presynaptic membrane, releasing neurotransmitters and neuropeptides that activate postsynaptic ion channels and G protein coupled receptors (GPCRs) (Betke et al., 2012; Geppetti et al., 2015). While much has been learned about neurotransmitter signaling pathways through ionotropic receptors, the diversity of GPCRs and their signaling pathways has complicated our understanding of how their signaling exerts changes on cell excitability and behavior. The G protein, $G\alpha_q$, is one of the major G proteins expressed in all excitable cells (Offermanns, 2001; Simon et al., 1991; Wilkie et al., 1992). Activated $G\alpha_q$ signals through PIP_2-specific Phospholipase-Cβ (PLCβ) to generate the second messengers, inositol 1,4,5 trisphosphate (IP_3) and 1,2-diacylglycerol (DAG). IP_3 activates the IP_3 receptor to release Ca^{2+} from intracellular stores and activate downstream kinases, lipases, and ion channels (Berridge et al., 2000; Huang, 1989; Li et al., 2014; Mujica and Gonzalez, 2011). The membrane lipid DAG has been shown to recruit and activate numerous effector proteins including UNC-13 and Protein Kinase C (Ananthanarayanan et al., 2003; Brose and Rosenmund, 2002; Lou et al., 2008; Maruyama and Brenner, 1991; Rozengurt et al., 1997; Silinsky and Searl, 2003; Thore et al., 2005), but whether these or other identified DAG targets function to transduce all forms of $G\alpha_q$ signaling *in vivo* remains an open question.

Genetic studies in the nematode worm *C. elegans* show that $G\alpha_q$ signaling through both PLCβ and Trio promotes neurotransmitter and neuropeptide transmission. In *C. elegans unc-73* gene encodes at least 8 isoforms of Trio, which has both Rac and Rho GTPase exchange factor (GEF) DH/PH domains (Steven et al., 2005; Williams et al., 2007). *unc-73* mutations that specifically affect the second Rho activating DH/PH GEF domain of Trio (Trio RhoGEF) disrupt locomotion, feeding, and egg-laying behaviors (Williams et al., 2007), without causing the axon

53 pathfinding and neurodevelopmental defects observed in animals bearing *unc-73* Trio RacGEF
54 mutations that affect the first, Rac activating DH/PH GEF domain (Steven et al., 1998). In worms,
55 $G\alpha_q$ knockouts are lethal while PLCβ or Trio RhoGEF single knockouts show defects in
56 neurotransmission that disrupt locomotion, feeding, egg-laying and other behaviors, resembling
57 $G\alpha_q$ loss-of-function mutants (Bastiani et al., 2003; Brundage et al., 1996; Hajdu-Cronin et al.,
58 1999; Lackner et al., 1999). Worms bearing mutations that disrupt both PLCβ and Trio RhoGEF
59 phenocopy the larval arrest phenotype of $G\alpha_q$ null mutants, consistent with these two effectors
60 relaying most or all of the relevant $G\alpha_q$ signaling (Williams et al., 2007). Genetic and biochemical
61 studies showed that $G\alpha_q$ binding to and activation of the Trio RhoGEF domain to promote Rho
62 signaling is conserved in mammals (Chhatriwala et al., 2007; Rojas et al., 2007), however, it
63 remains unclear how PLCβ and Rho signaling promotes neurotransmitter and neuropeptide
64 release *in vivo*. The larval lethality of $G\alpha_q$ null mutants can be rescued by the DAG-mimetic
65 phorbol ester, PMA (Reynolds et al., 2005), and PMA can also rescue the egg-laying defects of
66 PLCβ, Trio RhoGEF double mutants (Williams et al., 2007). These results suggest $G\alpha_q$ signaling
67 through both PLCβ and Trio may ultimately converge to regulate DAG levels and the activation
68 of downstream effectors. Both PLCβ and Trio RhoGEF promote acetylcholine (ACh) release
69 from motor neurons that control locomotion (Lackner et al., 1999; Miller et al., 1999; Williams et
70 al., 2007), although mutations in Trio RhoGEF cause behavior defects more aligned with a
71 function in dense core vesicle release (Hu et al., 2011). $G\alpha_q$, Trio, and PLCβ are expressed in
72 the nervous system and in muscles (Bastiani et al., 2003; Lackner et al., 1999; Steven et al.,
73 1998; Steven et al., 2005; Taylor et al., 2021). While re-expression of PLCβ in motor neurons
74 (Lackner et al., 1999) or Trio in all neurons (Williams et al., 2007) rescues the locomotion
75 behavior defects of their mutants, prior work has shown that $G\alpha_q$ has additional functions to
76 promote egg laying in muscles (Bastiani et al., 2003) where Trio RhoGEF is also expressed

77 (Steven et al., 2005). Loss of PLCβ fails to suppress the hyperactive egg-laying phenotypes of
78 $G\alpha_q$ gain-of-function mutants, consistent with $G\alpha_q$ signaling through other effectors like Trio
79 RhoGEF to regulate egg laying (Bastiani et al., 2003). Indeed, *unc-73* RhoGEF mutations
80 strongly suppress the hyperactive egg-laying behavior phenotypes of $G\alpha_o$ mutants unable to
81 inhibit $G\alpha_q$ signaling (Williams et al., 2007).

82 Using genetics, optogenetics, pharmacology, and Ca^{2+} imaging techniques we have
83 investigated how $G\alpha_q$ and its two effector pathways regulate egg-laying circuit activity and
84 behavior. We find that PLCβ functions in the neurons while Trio RhoGEF signals in both neurons
85 and muscles to promote egg laying. Loss of each of these effectors imparts specific defects in
86 egg-laying behavior that indicate these proteins function in distinct cells to promote egg-laying
87 circuit activity and behavior. Many of these defects can be rescued in part by treatment with
88 phorbol esters that mimic DAG production. Thus, despite $G\alpha_q$ signaling through independent
89 PLCβ and Trio RhoGEF pathways, these effectors may ultimately converge to increase DAG
90 levels which promote egg-laying behavior.

91 **MATERIALS AND METHODS**

92 **Strains**

93 *C. elegans* worms were maintained at 20 °C on Nematode Growth Medium (NGM) agar plates
94 with *E. coli* OP50 as a source of food as described previously (Brenner, 1974). All behavior
95 assays and fluorescence imaging experiments were performed with age-matched adult
96 hermaphrodites aged 24-36 h after the late L4 stage. Strains used in this study are listed in Table
97 1.

98

99 **Molecular biology and transgenes**

100 **Vulval muscle GCaMP5 strains**

101 Vulval muscle Ca^{2+} activity was recorded using GCaMP5G (Akerboom et al., 2013) which was
102 expressed along with mCherry from the *unc-103e* promoter (Collins and Koelle, 2013), as
103 previously described (Collins et al., 2016; Ravi et al., 2018a). The wild-type reporter strain,
104 LX1918 *vsIs164 [unc-103e::GCaMP5::unc-54 3'UTR + unc-103e::mCherry::unc-54 3'UTR + lin-*
105 *15(+)] lite-1(ce314) lin-15(n765ts) X* was described previously (Collins et al., 2016). LX1918
106 males were crossed separately into DA823 *egl-30(ad805) I*, MT1434 *egl-30(n686) I*, JT47 *egl-*
107 *8(sa47) V*, MT1083 *egl-8(n488) V*, KG1278 *unc-73(ce362) I*, LX1226 *eat-16(tm761) I*, CG21 *egl-*
108 *30(tg26) I*, *him-5(e1490) V*, or KP1097 *dgk-1(nu62) X* hermaphrodites to generate MIA140 *egl-*
109 *30(ad805) I; vsIs164 lite-1(ce314) lin-15(n765ts) X*, MIA139 *egl-30(n686) I; vsIs164 lite-1(ce314)*
110 *lin-15(n765ts) X*, MIA109 *egl-8(sa47) V; vsIs164 lite-1(ce314) lin-15(n765ts) X*, MIA288 *egl-*
111 *8(n488) V; vsIs164 lite-1(ce314) lin-15(n765ts) X*, MIA141 *unc-73(ce362) I; vsIs164 lite-1(ce314)*
112 *lin-15(n765ts) X,* MIA287 *eat-16(tm761) I; vsIs164 lite-1(ce314) lin-15(n765ts) X*, MIA286 *egl-*
113 *30(tg26) I; vsIs164 lite-1(ce314) lin-15(n765ts) X* ,and MIA296 *dgk-1(nu62) vsIs164 lite-1(ce314)*
114 *lin-15(n765ts) X*, respectively. The corresponding gene mutation was confirmed by phenotype,
115 genotype, or both. Presence of *vsIs164* was confirmed observing the mCherry marker, and *lite-*

116 *1(ce314) X* was confirmed with PCR genotyping. Oligo sequences used for genotyping the
117 corresponding mutations are shown in Table 2.
118
119 **Trio RhoGEF-E transgenes**
120 *Pan-neuronal expression*:
121 The *rab-3* promoter was used to drive expression of GFP alone or with Trio-RhoGEF-E. Briefly,
122 plasmids KG#68 (*rab-3p::GFP*; 15 ng/µl) alone or with KG#281 (*rab-3p:: unc-73e;* 50 ng/µL)
123 were injected into KG1278 *unc-73(ce362) I* (Williams et al., 2007). For behavior experiments,
124 five independent GFP-expressing transgenic lines were used, from which a single transgenic
125 line from each was kept: MIA374 *unc-73(ce362) I*; *keyEx66* (expressing GFP alone) and MIA375
126 *unc-73(ce362) I*; *keyEx67* (expressing GFP and Trio RhoGEF-E). Plasmids KG#281(*rab-*
127 *3p::unc-73e*) and KG#68(*rab-3p::GFP*) were kind gifts from Dr. Kenneth Miller.
128
129 *Pan-muscle expression*
130 Plasmid pKMC33 (*rgs-1p::mCherry*) was digested with NheI/KpnI and ligated with similarly
131 digested pPD96.52 (Fire lab *C. elegans* Vector Kit 1999; 1608: L2534, Addgene) to generate
132 pKMC166 (*myo-3p::mCherry*). Plasmid KG#281 (*rab-3p::unc-73e*) was digested with NheI and
133 KpnI, and the insert was ligated into similarly digested pKMC166 to generate pPD3 (*myo-*
134 *3p::unc-73e*). pKMC166 (15 ng/µL) alone or with pPD3 (50 ng/µL) was injected into KG1278
135 *unc-73(ce362) I* mutants. Five independent mCherry-expressing transgenic lines were used for
136 behavior experiments from which a single transgenic line from each was kept: MIA376 *unc-*
137 *73(ce362) I; keyEx68* (expressing mCherry alone) and MIA377 *unc-73(ce362) I*; *keyEx69*
138 (expressing mCherry + Trio RhoGEF-E).
139
140 Neuron and muscle co-expression

141 Plasmids KG#68 (15 ng/µl; pan-neuronal GFP) or pKMC166 (15 ng/µl; pan-muscle mCherry)
142 alone or with KG#281 (50ng/µl; pan-neuronal *unc-73e*) and pPD3 (50ng/µL; pan-muscle *unc-*
143 *73e*) were injected into KG1278 *unc-73(ce362) I*, generating five independent mCherry(+),
144 GFP(+) transgenic lines for behavior experiments from which a single transgenic line from each
145 was kept: MIA372 *unc-73(ce362); keyEx64* expressing mCherry (muscles) and GFP (neurons)
146 only and MIA373 *unc-73(ce362); keyEx65* expressing GFP (neurons), mCherry (muscles) and
147 TrioRhoGEF-E (both neurons and muscles).
148

149 **PLCβ Transgenes**

150 To generate a control plasmid expressing GFP in neurons, GFP coding sequences were
151 amplified from pJM60 (Moresco and Koelle, 2004) using oligonucleotides RE-GFP-FWD / -REV,
152 digested with NheI / KpnI, and ligated into similarly digested pGP3 bearing the *rgs-1* promoter
153 (Dong et al., 2000), generating pKMC78. An *egl-8* cDNA was used to generate and express a
154 functional GFP fusion protein in neurons. Briefly, oligonucleotides egl-8-cDNA-fwd / -rev were
155 used to amplified *egl-8* coding sequences from a plasmid bearing an *egl-8* cDNA provided by
156 Dr. Kenneth Miller (pKP309). This amplicon was digested with NheI / NcoI and ligated into a
157 similarly digested pPD49.26 plasmid, generating pKMC193. Quickchange mutagenesis with
158 oligonucleotides egl-8-Cterm-NotI-fwd / -rev were used to insert an in-frame NotI site near the 3'
159 end of the *egl-8* cDNA in a divergent region of the coding sequence, generating plasmid
160 pKMC194. Coding sequences for *egl-8* bearing this NotI site were then moved to pKMC78 by
161 digestion of pKMC194 with NheI/NcoI followed by ligation into a similarly digested pKMC78,
162 generating pKMC195. Oligonucleotides NotI-GFP-FWD / -REV were used to amplified GFP
163 coding sequences from pKMC78, digested with NotI, and ligated into a similarly digested
164 pKMC195, generating pKMC196. A strain bearing the *egl-8(sa47)* mutation was generously
165 provided by Dr. Joshua Kaplan and backcrossed four times to N2 wild-type animals to generate

166 LX1225 *egl-8(sa47) V.* MT8189 *lin-15(n765ts)* males were mated to LX1225 to generate LX1287
167 *egl-8(sa47) V; lin-15(n765ts) X* hermaphrodites that were kept at 15°C prior to injection.
168 Plasmids expressing GFP alone (pKMC78; 5 ng/µl) or *egl-8* CDNA fused to GFP (pKMC196; 5
169 ng/µl) from the *rgs-1* promoter were injected along with pL15EK (50 ng/µl) into LX1287
170 hermaphrodites. For behavior experiments, five independent GFP-expressing lines were used
171 from which a single transgenic line (*vsEx679* [GFP] and *vsEx680* [EGL-8::GFP], respectively)
172 was kept. We noted that transgenic expression of GFP alone did cause a modest, but significant
173 reduction of egg accumulation compared to LX1225 *egl-8(sa47) V* mutant animals. This effect
174 appeared to be specific for egg accumulation, as these same *egl-8(sa47)* GFP-only expressing
175 transgenic lines showed similar resistance to 1 mM aldicarb as LX1225 *egl-8(sa47) V* (0 ±2.1%
176 vs. 9 ±5.9% of animals paralyzed at 4 h, respectively). In contrast, 48 ± 7.9% of transgenic *egl-*
177 *8(sa47)* animals expressing EGL-8::GFP were paralyzed at 4 h, not significantly different to wild-
178 type N2 animals (51 ±9.6% of animals paralyzed at 4 h).
179

180 **Vulval muscle Channelrhodopsin-2 strains**

181 N2 males were crossed into MIA229 *keyIs48 [ceh-24p::ChR2::unc-54 3'UTR + lin-15(+)], lite-*
182 *1(ce314), lin-15(n765ts) X* (Kopchock et al., 2021) to produce F1 heterozygous males, which
183 then were crossed separately into MIA211 *unc-73(ce362) I; lite-1(ce314) lin-15(n765ts) X,*
184 MIA299 *egl-30(ad805) I; lite-1(ce314) lin-15(n765ts) X*, MIA303 *egl-8(n488) V; lite-1(ce314) lin-*
185 *15(n765ts) X*, or MIA307 *egl-8(sa47) V; lite-1(ce314) lin-15(n765ts) X* hermaphrodites to
186 generate vulval muscle specific Channelrhodopsin-2 (ChR2) expressing transgenic lines
187 MIA248 *unc-73(ce362) I; keyIs48; lite-1(ce314) X*, MIA301 *egl-30(ad805) I; keyIs48; lite-*
188 *1(ce314) X*, MIA305 *egl-8(n488) V; keyIs48; lite-1(ce314) X*, and MIA309 *egl-8(sa47) V;*
189 *keyIs48; lite-1(ce314) X*, respectively. The presence of *lite-1(ce362)* was confirmed by

190 genotyping as above, and the presence of the ChR2 transgene was confirmed by rescue of the
191 *lin-15(n765ts)* multi-vulva (Muv) phenotype.
192
193 **HSN Channelrhodopsin-2 strains**
194 ChR2 was expressed in the HSNs from the *egl-6* promoter via an integrated *wzIs30* transgene
195 (Emtage et al., 2012). This transgene was crossed into $G\alpha_q$ signaling mutants as follows. N2
196 males were crossed into LX1836 *wzIs30 IV; lite-1(ce314) lin-15(n765ts) X* to generate
197 heterozygous F1 males, which were then crossed separately into MIA211 *unc-73(ce362) I; lite-*
198 *1(ce314) lin-15(n765ts) X,* MIA299 *egl-30(ad805) I; lite-1(ce314) lin-15(n765ts) X*, MIA303 *egl-*
199 *8(n488) V; lite-1(ce314) lin-15(n765ts) X,* or MIA307 *egl-8(sa47) V; lite-1(ce314) lin-15(n765ts)*
200 *X* hermaphrodites to generate MIA247 *unc-73(ce362) I; wzIs30 IV; lite-1(ce314) X,* MIA300 *egl-*
201 *30(ad805) I; wzIs30 IV; lite-1(ce314) X*, MIA304 *wzIs30 IV; egl-8(n488)V; lite-1(ce314) X*, and
202 MIA308 *wzIs30 IV; egl-8(sa47) V; lite-1(ce314) X*, respectively. The presence of *lite-1(ce362)*
203 was confirmed by PCR genotyping, and the *wzIs30* transgene was confirmed by rescue of the
204 *lin-15(n765ts)* Muv phenotype.
205
206 **Other strains**
207 A single-copy MosSCI knock-in strain expressing *unc-103* bearing the *e1597dm* gain-of-function
208 mutation was constructed as described (Collins and Koelle, 2013). Briefly, plasmid pKMC179
209 bearing *unc-103* coding sequences behind the *unc-103e* promoter/enhancer was mutagenized
210 by QuickChange using primers unc-103(gf)-QC-fwd and unc-103(gf)-QC-rev to generate
211 pKMC183. Digestion with BsrGI and Sanger sequencing confirmed the mutagenesis was
212 successful. *Unc-103(e1597gf)* coding sequences were then PCR-amplified from pKMC183
213 using Phusion polymerase (NEB), digested with NheI/MluI enzymes, and then ligated into
214 pKMC176, a *ttTi5606* site MosSCI donor plasmid, generating pKMC185. pKMC185 was then

injected at 50 ng/µl along with plasmids expressing Mos1 transposase and mCherry co-injection markers into EG4322 *ttTi5605 II; unc-119(ed9) III*, as described (Frokjaer-Jensen et al., 2008), generating LX1565 *vsSi3[Punc-103e::unc-103e(e1597dm)-GFP, cb-unc-119(+)] II*; *unc-119(ed3) III* which had a strong Egl phenotype but markedly reduced Unc phenotype compared to the reference CB1597 *unc-103(e1597dm)* strain. LX1565 was then outcrossed to N2 four times to generate LX1615 *vsSi3[Punc-103e::unc-103e(e1597dm)-GFP, cb-unc-119(+)] II*.

Behavior assays

Quantification of egg accumulation was performed as described (Chase and Koelle, 2004). Staged adults were obtained by picking late L4 animals and culturing them 24-30 h at 20 °C. Each animal was placed in 7 µL of 20% hypochlorite (bleach) solution and eggs were counted after animals had dissolved. Numbers of eggs and any internally hatched L1 animals were combined.

Pharmacological assays

Egg laying in response to exogenous serotonin was performed as described (Banerjee et al., 2017; Kopchock et al., 2021). Individual staged adult animals were placed in 100 µl of either M9 buffer alone, or M9 containing 18.5 mM serotonin (creatinine sulfate monohydrate salt, Sigma-Aldrich #H7752) or M9 containing 10 µM PMA (Phorbol-12-myristate-13-acetate, Calbiochem #524400) in a 96-well microtiter dish. After 1 hour, the number of released eggs and L1 larvae in each well were counted. Since egg-laying defective animals sometimes release one or two eggs/L1 larvae when they are first picked into the well in response to mechanical stimulation, animals were only recorded as responding if they laid 3 or more progeny. For Ca^{2+} imaging, NGM plates containing either PMA or ethanol solvent were prepared as described (Reynolds et al., 2005). Age-matched adult worms from each genotype were placed on separate PMA or

240 control NGM plates at room temperature for 1.5 hours. An agar chunk was then placed between
241 two glass coverslips for Ca^{2+} activity recording as described (Ravi et al., 2018b). The unused
242 plates were kept at 4 °C for future use.
243

244 **Optogenetic assay**

245 All-*trans* retinal (Sigma Aldrich, R2500) was resuspended in ethanol (100%) to make 100 mM
246 solution and added to a warmed culture of OP50 bacteria grown in B Broth media to a final
247 concentration of 0.4 mM. Individual NGM agar plates were seeded with 200 µl of freshly
248 prepared +ATR food and were grown in the dark for ~24 hours prior to use. In all photo-
249 stimulation experiments, a set of control animals were grown in the absence of ATR. Animals
250 were imaged at 4x magnification on a Leica M165FC stereomicroscope and illuminated with 3.3
251 mW/cm^2 of ~470 ± 20 nm blue light produced using a EL6000 metal halide light source and a
252 GFP excitation/emission filter set. The 30 s on/off sequence was programmed and controlled
253 using a Doric Optogenetics TTL Pulse Generator (OTPG-4, Version 3.3) triggering a SHB1
254 series shutter controller (ThorLabs; 170712-1).
255

256 **Microscopy**

257 **Ratiometric Ca^{2+} imaging**

258 Vulval muscle Ca^{2+} activity was performed in freely behaving adult animals at 24-30 h past the
259 late L4 larval stage, as described previously (Collins et al., 2016; Collins and Koelle, 2013; Ravi
260 et al., 2018a). Worms co-expressing GCaMP5G and mCherry under the *unc-103e* promoter
261 transgene *vsIs164* were mounted beneath the chunk of agar over the glass coverslip, and
262 reporter fluorescence was recorded through an 20X Apochromatic objective (0.8 NA) mounted
263 on an inverted Zeiss Axio Observer.Z1. A Colibri.2 LED illumination system was used to excite
264 GCaMP5 at 470 nm and mCherry at 590 nm for 10 msec every 50 msec. GFP and mCherry

265 fluorescence emission channels were separated using a Hamamatsu W-VIEW Gemini image
266 splitter and recorded simultaneously for 10 min with an ORCA-Flash 4.0 V2 sCMOS camera at
267 256 / 256-pixel resolution (4x4 binning) at 16-bit depth. A motorized stage was manually
268 controlled using a joystick to maintain the freely behaving animal in the field of view. For
269 experiments without treatment of PMA or vehicle control, animals were recorded until each
270 entered into an egg-laying active state. The recording was then cropped to a 10 minute (12,000
271 frame) two channel image sequence, centered on the first egg-laying event observed, for
272 subsequent ratiometric analysis. The egg-laying active state was operationally defined as
273 starting 1 minute before the first egg-laying event and ending 1 minute after the last egg-laying
274 event observed in the 10 min recording. For egg-laying defective mutants like *egl-30(ad805)* and
275 *unc-73(ce362)* that lay essentially no eggs, the 10 min extraction was not centered on any
276 specific behavioral feature. For drug and vehicle control assays, the 10 min recording period
277 started immediately, whether or not animals laid eggs or were seen to enter into an active state.
278 Image sequences were exported to Volocity software (Quorum Technologies Inc.) for
279 segmentation and ratiometric analysis. Ca^{2+} transient peaks from ratio traces were detected
280 using a custom MATLAB script, as described (Ravi et al., 2018b).
281

282 **Experimental design and statistical analysis**

283 Sample sizes for behavioral assays followed previous studies (Chase and Koelle, 2004; Collins
284 et al., 2016). Statistical analysis was performed using Prism v.8 or v.9 (GraphPad). Ca^{2+}
285 transient peak amplitudes, widths, and inter-transient intervals were pooled from multiple
286 animals (typically ≥10 animals per genotype). All statistical tests were corrected for multiple
287 comparisons (Bonferroni for one-way ANOVA or Fisher's exact tests; Dunn's correction for
288 Kruskal–Wallis tests). Each figure legend indicates individual p-values with $p<0.05$ being
289 considered significant.

290 **Data Availability statement**

291 All the data, reagents, and strains used in this study are available from the corresponding author

292 upon request.

Results

Trio RhoGEF acts in both neurons and muscles to drive egg-laying behavior

Prior studies have shown that $G\alpha_q$ signaling (Fig. 1A) through PLCβ and Trio RhoGEF promotes neurotransmitter release and locomotion (Brundage et al., 1996; Miller et al., 1999; Williams et al., 2007). How $G\alpha_q$ signaling regulates other *C. elegans* behavior circuits is less well established. To address this uncertainty, we chose to examine the neural circuit driving egg-laying behavior. Egg-laying behavior in *C. elegans* is regulated by a small motor circuit with defined neurons and muscle connectivity (Cook et al., 2019; White et al., 1986). The HSNs are serotonergic command motor neurons (Fig. 1B) that initiate the egg-laying active state and promote the excitability of the vm1 and vm2 egg-laying vulval muscles (Collins et al., 2016; Emtage et al., 2012; Waggoner et al., 1998). Innervating ventral cord motor neurons release acetylcholine to regulate muscle contraction (Bany et al., 2003; Kim et al., 2001; Kopchock et al., 2021; Waggoner et al., 2000). We first examined the steady-state accumulation of eggs in the uterus as a proxy for changes in egg-laying circuit activity and behavior. As previously shown, animals bearing mutations in the EAT-16 RGS protein, which inhibits $G\alpha_q$ signaling (Hajdu-Cronin et al., 1999), or gain-of-function mutations in $G\alpha_q$ itself, (Bastiani et al., 2003; Doi and Iwasaki, 2002) showed a significant increase in egg laying resulting in a significant reduction in egg accumulation compared to the ~15 ± 1.4 embryos retained in wild-type animals (Fig. 1C-E; Fig. 1I). Conversely, animals bearing mutations which reduce $G\alpha_q$ signaling showed the opposite phenotype. Animals bearing an early nonsense mutation predicted to be a PLCβ null mutant, *egl-8(sa47),* (Lackner et al., 1999; Williams et al., 2007) accumulated an average of 21 eggs, showing a significant increase in egg retention (Fig. 1G). Animals bearing a missense mutation in the RhoGEF domain of Trio, *unc-73(ce362)* (Williams et al., 2007), showed an even stronger egg-laying behavior defect, accumulating more than 30 eggs in the uterus, closely resembling

317 animals bearing loss-of-function mutations in $G\alpha_q$ itself (Fig. 1F-1I). Together, these results
318 confirm that $G\alpha_q$ and its effectors PLCβ and Trio RhoGEF are required for egg-laying behavior
319 in *C. elegans* and that loss of the Trio RhoGEF branch causes a stronger behavior impairment
320 compared to loss of PLCβ.

321 Previous work has shown that $G\alpha_q$, Trio, and PLCβ are expressed in neurons and
322 muscles of the egg-laying circuit (Bastiani et al., 2003; Brundage et al., 1996; Lackner et al.,
323 1999; Miller et al., 1999; Steven et al., 1998; Taylor et al., 2021). To understand where $G\alpha_q$ and
324 its effectors function to regulate egg laying, we used tissue-specific promoters to express cDNAs
325 encoding PLCβ or Trio RhoGEF in either all neurons, in the body wall and egg-laying vulval
326 muscles, or in both neurons and muscles. We found that transgenic expression of PLCβ from
327 the pan-neuronal *rgs-1* promoter (Dong et al., 2000) in PLCβ null mutants was sufficient to
328 rescue their defects in egg laying (Fig. 1J) and acetylcholine (ACh) release as measured by
329 restoration of sensitivity to aldicarb, a cholinesterase inhibitor (see Methods). This suggests
330 PLCβ functions in neurons to regulate egg laying. Previous work has indicated the presence of
331 eight transcript variants of Trio (A, B, C1, C2, D1, D2, E, and F), which are differentially
332 expressed in *C. elegans* (Steven et al., 1998; Steven et al., 2005). Transgenic expression of Trio
333 RhoGEF-E in neurons is sufficient to rescue the locomotion defects of Trio RhoGEF mutants
334 (Williams et al., 2007). To explore whether Trio RhoGEF acts similarly in neurons to promote
335 egg laying, we used the *rab-3* pan-neuronal promoter (Williams et al., 2007) to express Trio
336 RhoGEF-E and measured egg accumulation in these animals. We observed a modest, but
337 significant reduction in the number of eggs retained in Trio RhoGEF mutants (~36 eggs)
338 compared to control Trio RhoGEF mutant animals (~42 eggs; Fig. 1K). Transgenic expression
339 of Trio RhoGEF-E in the egg-laying vulval muscles from a muscle-specific promoter showed a
340 greater rescue of egg accumulation (~25 eggs), and this rescue of egg laying was improved to
341 nearly wild-type levels when Trio RhoGEF-E was expressed in both neurons and muscles (~19

342 eggs; Fig. 1K). Although these rescue lines are extrachromosomal arrays and likely expressed
343 at different levels and with different amounts of mosaicism, these results support a general
344 interpretation that *unc-73* functions in both neurons and muscles to promote egg laying.
345 However, because previous work showed that expression of *unc-73* in neurons can rescue
346 locomotion defects (Williams et al., 2007) but not egg laying (Fig. 1K and data not shown), these
347 results indicate that *unc-73* has additional functions in muscle that cannot be bypassed or
348 rescued by expression just in neurons. Together, these results suggest that $G\alpha_q$ effectors PLCβ
349 and Trio RhoGEF function in neurons to regulate egg-laying behavior. Our results also suggest
350 Trio RhoGEF also functions in the postsynaptic vulval muscles for proper regulation of egg
351 laying, a finding consistent with previously results regarding $G\alpha_q$ (Bastiani et al., 2003).
352

353 **Serotonin signals through $G\alpha_q$, Trio, and PLCβ to promote egg laying.**

354 Previous studies have shown that serotonin released from the HSNs signals through G-protein
355 coupled serotonin receptors expressed on the vulval muscles (Bastiani et al., 2003; Dempsey et
356 al., 2005; Fernandez et al., 2020; Tanis et al., 2008; Xiao et al., 2006). The vulval muscles are
357 also innervated by cholinergic ventral cord motor neurons (Cook et al., 2019; White et al., 1986)
358 whose release of ACh is regulated by serotonin and G protein signaling (Nurrish et al., 1999).
359 To test how serotonin promotes egg laying via $G\alpha_q$, we measured the egg-laying response to
360 serotonin in $G\alpha_q$ signaling mutants. Serotonin promotes egg laying in hypertonic M9 buffer, a
361 condition that normally inhibits egg laying in both wild-type and HSN-deficient *egl-1(n986dm)*
362 mutants, which developmentally lack the HSNs (Fig. 2B). Consistent with previous results
363 (Bastiani et al., 2003; Brundage et al., 1996; Trent et al., 1983), more than 62% of wild-type
364 animals and 57% of HSN-deficient *egl-1(n986dm)* mutant animals laid eggs in response to
365 serotonin compared to only 13% of $G\alpha_q$ mutant animals (Fig. 2B). Serotonin response was

366 similarly and significantly reduced to 23% and 3% in PLCβ and Trio RhoGEF mutant animals,
367 respectively (Fig. 2B). Our results are consistent with the previous data reporting that $G\alpha_q$ loss-
368 of-function mutants and the PLCβ deletion mutant, *egl-8(n488)* do not lay eggs in response to
369 exogenous serotonin (Bastiani et al., 2003; Trent et al., 1983).

370 To confirm whether PLCβ is required for egg laying in response to serotonin, we tested
371 other PLCβ mutants including *sa47* and *md1971*, both of which carry nonsense mutations
372 predicted to terminate the protein prematurely, and *e2917* in which the coding sequence is
373 disrupted by a Mos1 transposon (Lackner et al., 1999; Miller et al., 1999; Yook and Hodgkin,
374 2007). All PLCβ mutants tested failed to lay eggs in response to exogenous serotonin after 60
375 min (Fig. 2B), but only *egl-8(n488)* animals remained resistant to serotonin after 90 minutes
376 (Table 3), with the other PLCβ mutant animals beginning to lay eggs by 90 minutes, consistent
377 with previous observations (Bastiani et al., 2003). Taken together, these results indicate that
378 $G\alpha_q$, PLCβ, and Trio act at least in part outside of HSNs to promote egg laying in response to
379 serotonin. To determine where in the animal the Trio RhoGEF deficiency caused serotonin
380 insensitivity, we measured egg laying in Trio RhoGEF mutant animals re-expressing Trio
381 RhoGEF-E in either neurons, muscles, or both. Transgenic expression of Trio RhoGEF-E in
382 neurons failed to rescue egg laying in response to serotonin (Fig. 2C), but expression of Trio
383 RhoGEF-E in muscles, or in both neurons and muscles, restored egg laying of *unc-73(ce362)*
384 mutant animals (Fig. 2C), suggesting Trio RhoGEF mediates serotonin signaling by acting in the
385 vulval muscles. Together, these results indicate that $G\alpha_q$, PLCβ, and Trio RhoGEF function at
386 least in part outside of the HSNs to drive egg laying in response to serotonin with Trio RhoGEF
387 likely functioning in the muscles.

388

389 **Optogenetic stimulation of the HSNs and vulval muscles suggests cellular specificity of**
390 **$G\alpha_q$ effectors for egg-laying.**

391 Optogenetic stimulation of Channelrhodopsin-2 (ChR2) expressed in either the HSNs (Emtage
392 et al., 2012) or vulval muscles (Kopchock et al., 2021) can drive egg laying. To test whether and
393 how $G\alpha_q$ and its effectors mediate this response, we expressed ChR2 in HSNs in $G\alpha_q$ and
394 effector mutants and measured egg laying during 30s of exposure to blue light. Blue light
395 stimulation of the HSNs drove an average release of ~3 eggs in wild-type animals, which was
396 reduced to essentially zero in $G\alpha_q$ [(*egl-30(ad805)*] and Trio RhoGEF [*unc-73(ce362)*] mutants
397 (Fig. 3A), consistent to our previous results showing Trio RhoGEF acts in part downstream of
398 the HSNs in the postsynaptic vulval muscles. In contrast, optogenetic stimulation of the HSNs in
399 PLCβ null mutants [*egl-8(sa47)* or *egl-8(n488)*] drove robust egg release, releasing an average
400 of ~4 and ~6 embryos respectively in 30 s (Fig. 3A). To test whether the failure of egg laying in
401 $G\alpha_q$ and Trio RhoGEF mutants was a consequence of muscle developmental defects, rather
402 than excitability deficits, we expressed and stimulated ChR2 in the vulval muscles. Blue light
403 exposure drove the release of ~4 eggs in 30 s in wild-type animals. Both PLCβ [*egl-8(sa47)* and
404 *egl-8(n488)*] and Trio RhoGEF mutants [*unc-73(ce362)*] laid a similar number of eggs as wild-
405 type control animals after blue light stimulation (Fig. 3B). The *egl-30(ad805)* $G\alpha_q$ mutant laid
406 slightly fewer eggs on average (~3) but this was not significant. Thus, the failure of $G\alpha_q$ and Trio
407 mutants to lay eggs in response to exogenous serotonin or optogenetic stimulation of the HSNs
408 does not arise from some intrinsic defect in vulval muscle contractility, but rather a specific
409 deficiency in muscle excitability. These results are also consistent with prior findings showing
410 rescue of egg-laying behavior defects of $G\alpha_q$, PLCβ, and Trio RhoGEF mutants by exogenous
411 phorbol esters (Lackner et al., 1999; Williams et al., 2007).

412 Collectively, we interpret the previous serotonin experiments and these optogenetic
413 results as showing that $G\alpha_q$ signals through PLCβ in HSN and/or in other neurons to promote
414 release of neurotransmitters that signal through vulval muscle receptors coupled to $G\alpha_q$ and Trio

415 RhoGEF. That HSN optogenetic stimulation, but not exogenous serotonin, stimulates egg laying
416 in PLCβ mutants suggests HSN releases other factors such as NLP-3 neuropeptides (Brewer et
417 al., 2019) which signal to promote egg laying in parallel to serotonin and PLCβ. Our data do not
418 support a model where PLCβ acts only in HSNs as *egl-1(n986dm)* animals lacking HSNs still lay
419 eggs in response to serotonin while *egl-8* PLCβ null mutants do not (Fig. 2B). Together, these
420 results support the conclusion from our rescue experiments (Fig. 1J-1K) that PLCβ and Trio
421 RhoGEF function in distinct cells and through unique mechanisms to promote egg-laying circuit
422 activity and behavior.
423

424 **$G\alpha_q$ and Trio RhoGEF are required for vulval muscle Ca^{2+} activity**

425 Egg laying is a two-state behavior where ~20 minute inactive states are punctuated by ~2-minute
426 active states with high levels of rhythmic Ca^{2+} transient activity in the egg-laying circuit driving
427 release of 3-5 eggs (Collins et al., 2016; Waggoner et al., 1998; Zhang et al., 2008; Zhang et al.,
428 2010). Loss of $G\alpha_q$ signaling in *egl-30(n686)* animals causes a significant reduction in
429 spontaneous and serotonin-induced vulval muscle Ca^{2+} transients in immobilized animals (Shyn
430 et al., 2003). We therefore tested whether these $G\alpha_q$ dependent Ca^{2+} activity defects were
431 similarly seen in freely behaving animals on solid media and whether they were shared in PLCβ
432 and Trio RhoGEF mutants. We expressed the genetically encoded Ca^{2+} reporter, GCaMP5,
433 along with mCherry in the vulval muscles of mutant animals with either too much or too little $G\alpha_q$
434 signaling and performed ratiometric imaging as they entered and left the egg-laying active state.

435 As shown in Figure 4A, the normal two-state pattern of rhythmic vulval muscle Ca^{2+}
436 activity (and egg laying) is lost in animals bearing strong loss-of-function $G\alpha_q$ or Trio RhoGEF
437 mutations. To further quantify these activity defects, we compared vulval muscle Ca^{2+} transient
438 amplitudes and frequencies in wild-type and $G\alpha_q$ signaling mutant animals. In *egl-30(ad805)*

439 $G\alpha_q$ and *unc-73(ce362)* Trio mutants which laid no eggs during the recording period, we failed
440 to see the large amplitude egg-laying Ca^{2+} transients (1.4 ± 0.1 ΔR/R) typically observed in wild-
441 type animals where both the vm1 and vm2 muscles contract or even the smaller amplitude
442 rhythmic 'twitch' Ca^{2+} transients (0.4 ± 0.03 ΔR/R) that are localized primarily to the vm1 muscles
443 (Fig. 4A and 4B). As a result, the wild-type frequency of 3.5 ± 1.0 (ΔR/R) Ca^{2+} transients per min
444 was significantly reduced to essentially zero in *egl-30(ad805)* $G\alpha_q$ and *unc-73(ce362)* Trio
445 mutants (Fig. 4C). In contrast, we did not observe a significant reduction in the amplitude or
446 frequency of vulval muscle Ca^{2+} transients in *egl-30(n686)* $G\alpha_q$ weak loss-of-function mutants
447 or *egl-8(sa47)* and *egl-8(n488)* PLCβ null mutants compared to wild-type control animals (Fig.
448 4A-C). Such animals entered infrequent active states but their rhythmic vulval muscle twitching
449 and egg-laying Ca^{2+} transients were grossly intact. In fact, inspection of Ca^{2+} traces suggested
450 an apparent *increase* in vulval muscle Ca^{2+} transient activity in *egl-30(n686)* $G\alpha_q$ and PLCβ
451 mutants (Fig. 4A) including a significant increase in the amplitude and frequency of twitch Ca^{2+}
452 transients in *egl-8(n488)* PLCβ mutant animals (Fig. 4B and 4C). This elevated vulval muscle
453 Ca^{2+} activity was reminiscent of that observed in *egl-1(n986dm)* animals lacking the HSNs
454 (Collins et al., 2016) as these animals still enter and leave infrequent egg-laying active states,
455 possibly driven by the stretch-dependent feedback of egg accumulation in the uterus (Ravi et
456 al., 2018a) which does not appear to act by modulating HSN activity (Ravi et al., 2021). These
457 data further indicate that the egg-laying defects of PLCβ mutants are not caused by a loss of
458 vulval muscle Ca^{2+} activity.

459 Increased $G\alpha_q$ signaling enhances vulval muscle activity. *egl-30(tg26)* or *eat-16(tm761)*
460 mutant animals with elevated $G\alpha_q$ signaling showed even stronger egg-laying Ca^{2+} transients
461 with average amplitude >2 ΔR/R, a significant difference (Fig. 4A and 4B). Ca^{2+} transients were
462 also significantly more frequent in *egl-30(tg26)* $G\alpha_q$ gain-of-function mutants (~7 transients per

463 min) and in *eat-16(tm761)* $G\alpha_q$ RGS protein loss-of-function mutants (~5 transients per min)
464 (Fig. 4C). DAG Kinase-θ (DGK-θ) is thought to antagonize DAG signaling by catalyzing its
465 conversion to phosphatidic acid (Fig. 1A). *dgk-1(nu62)* mutants lacking DGK-θ/DGK-1 have
466 increased neurotransmitter release and egg laying (Jose and Koelle, 2005; Miller et al., 1996;
467 Nurrish et al., 1999), likely through elevation of DAG levels and activation of effectors
468 downstream of $G\alpha_q$. Somewhat surprisingly, *dgk-1(nu62)* mutant animals did not show a
469 significant increase in vulval muscle Ca^{2+} transient amplitude or frequency (Fig. 4A-C). Like
470 PLCβ, DGK-1 is expressed in neurons (Nurrish et al., 1999), suggesting alterations of IP_3 and/or
471 DAG levels in neurons may affect the frequency of egg-laying active states without altering the
472 overall pattern or strength of vulval muscle Ca^{2+} activity within those active states. Indeed, *goa-*
473 *1(n1134)* mutants that reduce inhibitory $G\alpha_o$ signaling have hyperactive egg-laying behavior
474 defects that strongly resemble *dgk-1(nu62)* mutants without a significant increase in vulval
475 muscle Ca^{2+} activity (Ravi et al., 2021). Together, these results indicate $G\alpha_q$ and Trio RhoGEF,
476 but not PLCβ, are required for vulval muscle activity that drives twitching and egg-laying Ca^{2+}
477 transients during egg-laying active states.
478

479 **DAG mimetics restore muscle activity and egg laying to $G\alpha_q$ signaling mutants**

480 How does serotonin signaling through $G\alpha_q$ promote vulval muscle activity? Previous results have
481 shown that DAG mimetic phorbol esters restore locomotion and animal viability to $G\alpha_q$ null
482 mutants and restore egg laying in PLCβ, Trio RhoGEF double mutants (Williams et al., 2007).
483 However, the effects of phorbol esters on egg laying in single mutants was not clear, raising
484 questions as to whether PMA rescued egg laying downstream of PLCβ, Trio RhoGEF, or both
485 (Fig. 5A). We measured the egg-laying responses of wild-type animals and $G\alpha_q$ signaling
486 mutants to Phorbol 12-myristate 13-acetate (PMA). As shown in Figure 5B, 10 μM PMA

487 treatment strongly stimulated egg laying in wild-type animals and all mutants with reduced $G\alpha_q$
488 signaling (≥80% animals laying eggs). Like serotonin (Fig. 2B), PMA also rescued egg laying in
489 *egl-1(n986dm)* mutant animals lacking the HSNs (Fig. 5B), but only PMA rescued egg laying in
490 $G\alpha_q$ and effector signaling mutants. These results are consistent with PMA acting downstream
491 of both serotonin release from the HSNs and its subsequent signaling through $G\alpha_q$-coupled
492 receptors. To test whether PMA and DAG act upstream to modulate vulval muscle electrical
493 excitability, we also tested the PMA response in animals carrying mutations in voltage-gated
494 channels that reduce or block egg laying. Loss of L-type Ca^{2+} channel activity in *egl-19(n582)*
495 hypomorphic mutants impairs egg laying downstream of serotonin (Trent et al., 1983; Waggoner
496 et al., 1998), but we find *egl-19(n582)* mutant animals still lay eggs in response to 10 μM PMA
497 (Fig. 5B). The *n582* mutation alters but does not eliminate Ca^{2+} channel function (Gao and Zhen,
498 2011; Jospin et al., 2002), possibly explaining how PMA could still rescue egg-laying behavior.
499 Indeed, *tpa-1(k530)* mutants originally identified by their resistance to phorbol esters like PMA
500 show synthetic egg-laying defects when combined with *egl-19(n582)* (Waggoner et al., 1998).
501 We next tested gain-of-function K^+ channel mutants that block egg laying. Animals expressing
502 A383V gain-of-function EGL-23 K2P channels (Ben Soussia et al., 2019; Trent et al., 1983),
503 A331T gain-of-function UNC-103 ERG K+ channels (Collins and Koelle, 2013; Reiner et al.,
504 1999; Reiner et al., 2006), or A478V gain-of-function EGL-2 EAG channels (Weinshenker et al.,
505 1999) showed reduced egg laying in response to PMA (Fig. 5B). PMA-induced egg laying was
506 completely blocked in *egl-23* K2P gain-of-function mutants, and the PMA response was
507 significantly reduced in both *unc-103* ERG and *egl-2* EAG mutant animals compared to wild type
508 (Fig. 5B). Although these results do not rule out that phorbol esters like PMA may be stimulating
509 egg laying in a manner independent of its DAG mimetic effects, our data supports a model where
510 $G\alpha_q$ and Trio RhoGEF signal upstream of DAG to promote vulval muscle excitability and/or
511 contractility.

512 We next imaged how PMA affected vulval muscle Ca^{2+} activity. We performed 10-minute
513 GCaMP5 Ca^{2+} recordings of wild-type or $G\alpha_q$ signaling mutants after two hours of exposure to
514 10 μM PMA (Movies 1-3). Quantitation of Ca^{2+} transients showed that PMA significantly
515 increased vulval muscle Ca^{2+} activity in wild-type animals to 10±1.6 transients per minute from
516 an average 2±0.9 transients per min in vehicle-treated, wild-type animals (Fig. 5C-D and Movie
517 1). PMA also restored both rhythmic twitch and egg-laying Ca^{2+} transients to strong $G\alpha_q$ and
518 Trio RhoGEF signaling mutants, with Ca^{2+} transients frequencies increasing from essentially
519 0±0.8 transients per minute in vehicle-treated controls to 7±2 transients per minute after PMA
520 treatment, almost but not quite to the level of PMA-treated wild-type control animals (Fig. 5C-D
521 and Movies 2-3). Together, these studies show that DAG-mimetic phorbol esters restore muscle
522 excitability and contractility defects of $G\alpha_q$ and Trio RhoGEF mutants, suggesting DAG
523 production could be a major and necessary consequence of both $G\alpha_q$ and Trio RhoGEF
524 signaling.
525

526 **Phorbol esters promote egg laying independent of UNC-13 or single Protein Kinase C**
527 **isoforms**

528 How do phorbol esters like PMA rescue vulval muscle Ca^{2+} activity and egg laying? Previous
529 results have shown that DAG and PMA bind to C1 domain-containing proteins such as mUNC-
530 13/UNC-13 and Protein Kinase C (PKC) to regulate their activity (Betz et al., 1998; Huang, 1989;
531 Konig et al., 1985; Newton, 2001; Silinsky and Searl, 2003).To test if DAG regulates egg-laying
532 behavior through activation of UNC-13 or PKC, we tested whether mutants lacking these
533 proteins still have a robust serotonin and/or PMA egg-laying response (Fig. 6). Mutants that
534 eliminate axonal and synaptic UNC-13 show reduced egg laying, accumulating an average of
535 22 eggs compared to 15 seen in wild-type animals (Fig. 6A), like PLCβ mutants but significantly

536 fewer than the >30 eggs that accumulate in $G\alpha_q$ and Trio RhoGEF mutants (Fig. 1C-I). *unc-13*
537 mutants also resemble PLCβ mutants in their egg-laying response to serotonin and PMA. Egg
538 laying in *unc-13* mutants was stimulated by PMA but was resistant to serotonin (Fig. 6B). While
539 the serotonin resistance we observed for *unc-13* mutants after one hour differs from that seen
540 by Bastiani et al., 2003 at 90 minutes, we saw similar differences for the PLCβ mutants (Table
541 3). These results show that serotonin promotes egg laying through a PLCβ and UNC-13-
542 dependent pathway that may be distinct from the PMA-stimulated pathway.

543 To determine whether $G\alpha_q$ and Trio RhoGEF signaling through the PMA-responsive
544 pathway is mediated by Protein Kinase C, we analyzed egg accumulation in animals bearing
545 predicted null mutations in different PKC isoforms (Edwards et al., 2012; Hyde et al., 2011;
546 Okochi et al., 2005; Tabuse, 2002; Tabuse et al., 1989). The *C. elegans* genome encodes four
547 PKCs isoforms PKC-1, PKC-2, PKC-3, and TPA-1. PKC-1 has previously been shown to
548 promote neuropeptide transmission (Sieburth et al., 2007). While neuropeptides signal to
549 promote egg laying (Avery et al., 1993; Brewer et al., 2019; Jacob and Kaplan, 2003; Kass et
550 al., 2001), PKC-1 (nPKC-ε) null mutants showed a grossly normal egg accumulation of 14~17
551 eggs (Fig. 6C). Animals bearing predicted null mutants of novel and conventional PKCs such as
552 nPKCδ/θ (TPA-1) and cPKCα/β (PKC-2) orthologs also show no significant differences in egg
553 accumulation (Fig. 6C), suggesting that, unlike loss of $G\alpha_q$ or Trio RhoGEF signaling, disruption
554 of individual PKC signaling pathways do not strongly affect egg-laying behavior. We next tested
555 whether PKC mediates the egg-laying response to PMA. All the PKC single mutant animals laid
556 eggs in response to PMA except for *pkc-1(nj1)* (Fig. 6C). The *nj1* allele is predicted to be a
557 missense mutation that may lead to the expression of a mutant PKC protein with altered function
558 (Okochi et al., 2005). Indeed, previous experiments using this mutant have shown that *pkc-1(nj1)*
559 mutant animals have stronger behavior defects (Okochi et al., 2005; Ventimiglia and Bargmann,
560 2017), suggesting the mutant protein may be expressed and interfere cell signaling, possibly by

561 interfering with the function of other co-expressed PKC isoforms like TPA-1. Together, these
562 results support a model where $G\alpha_q$ and Trio RhoGEF signaling in the vulval muscles drives
563 elevation of DAG which activates targets like PKCs and/or other effectors to promote cell
564 electrical excitability for egg laying.
565

566 **Discussion**

567 In this study we explored the cellular and molecular specificity of $G\alpha_q$ effector signaling as it
568 regulates egg-laying circuit activity and behavior using molecular genetics, optogenetics,
569 pharmacology, and Ca^{2+} imaging techniques. We found that $G\alpha_q$ effectors PLCβ and Trio
570 RhoGEF differentially act in neurons and muscles to promote synaptic transmission and egg-
571 laying behavior, supporting a working model where $G\alpha_q$ signals through Trio RhoGEF in both
572 neurons and muscles while PLCβ functions outside of HSN to promote egg laying (Fig. 7).
573 Although $G\alpha_q$, PLCβ, and Trio RhoGEF mutants all fail to lay eggs in response to serotonin,
574 optogenetic stimulation of HSNs fully rescued egg laying in PLCβ but not $G\alpha_q$ or Trio RhoGEF
575 mutants. Recent work has shown that the HSNs release NLP-3 neuropeptides which can
576 promote egg laying even in *tph-1* mutants lacking serotonin (Brewer et al., 2019), possibly
577 explaining why optogenetic activation of HSNs rescues egg laying to PLCβ mutants even when
578 exogenous serotonin cannot. The HSNs are also predicted to release ACh (Pereira et al., 2015),
579 and nAChR receptors are expressed on the vulval muscles and can stimulate egg laying (Kim
580 et al., 2001; Waggoner et al., 2000). Because serotonin drives egg laying in animals lacking
581 HSNs but not in animals lacking PLCβ, and that expression of PLCβ is sufficient to rescue normal
582 egg laying, we propose working model (Fig. 7) where $G\alpha_q$ and PLCβ act in neurons other than
583 HSNs to promote release of neurotransmitters like ACh onto the vulval muscles to stimulate egg
584 laying. The cholinergic VA, VB, and VC neurons also innervate the vulval muscles alongside the
585 HSNs and express PLCβ (Cook et al., 2019; Taylor et al., 2021; White et al., 1986). Consistent
586 with this model, we have recently shown that blocking VC synaptic transmission reduces egg
587 laying in response to serotonin (Kopchock et al., 2021). Optogenetic stimulation of the VCs
588 (Kopchock et al., 2021) or VA/VB neurons (Kopchock, 2021) stimulates vulval muscle Ca^{2+}
589 activity, but the resulting Ca^{2+} activity is insufficient to drive the strong egg-laying contractions.

590 Because we find that mutations that increase $G\alpha_q$ signaling have stronger vulval muscle Ca^{2+}
591 transients, we propose that serotonin and NLP-3 released from HSN potentiates ACh release
592 from other motor neurons and promotes the electrical excitability and/or contractility of the vulval
593 muscles, converting rhythmic twitch Ca^{2+} transients into stronger egg-laying transients. Previous
594 studies have shown that Trio RhoGEF acts in neurons to regulate locomotion behavior (Hu et
595 al., 2011; Steven et al., 2005; Williams et al., 2007). Our studies show that transgenic Trio
596 RhoGEF expression in either neurons or muscles alone is insufficient to restore wild-type level
597 of egg-laying behavior, but expression in both is sufficient. These results mirror previously
598 published results for $G\alpha_q$ (Bastiani et al., 2003), further supporting a model where PLCβ and
599 Trio RhoGEF functions during locomotion and egg-laying behaviors are distinct.

600 How does $G\alpha_q$, PLCβ, and Trio-RhoGEF signaling promote egg-laying behavior? Earlier
601 studies have suggested that Rho ortholog RHO-1 in *C. elegans* regulates synaptic activity in a
602 mechanism that involves the G12 family protein GPA-12 (Hiley et al., 2006; Lutz et al., 2005).
603 Activated RHO-1 also directly binds to and inhibits the DGK-1 diacylglycerol kinase expressed
604 in neurons that signals to reduce DAG available to bind effectors (Hiley et al., 2006; McMullan
605 et al., 2006). Our data are consistent with the previous results reporting that $G\alpha_q$ signaling
606 regulates postsynaptic vulval muscle activity mainly through $G\alpha_q$-Trio pathway as $G\alpha_q$ and Trio
607 mutants show a similarly strong reduction in vulval muscle Ca^{2+} activity. Because muscle activity
608 defects in $G\alpha_q$ and Trio mutants can be restored by the DAG-mimetic PMA, we suggest that
609 insufficient levels of DAG are responsible for the circuit activity and behavior defects of $G\alpha_q$ and
610 Trio RhoGEF mutants. In the absence of PLCβ, how would parallel $G\alpha_q$ signaling through Trio
611 RhoGEF and RHO-1 generate DAG? Besides PLCβ (EGL-8), *C. elegans* expresses four other
612 PLC orthologs: PLCε (PLC-1), PLC-2, PLCγ (PLC-3), and PLCδ (PLC-4) (Vázquez-Manrique et
613 al., 2008). *In vitro* studies with cultured mammalian cells show that small G proteins like Rho can

614 bind to and activate PLCε (Seifert et al., 2008; Wing et al., 2003). Genetic and molecular
615 expression evidence in *C. elegans* suggests a model where PLCε is activated downstream of
616 $G\alpha_q$ and Rho to promote cell activity (Kunitomo et al., 2013; Taylor et al., 2021; Yu et al., 2013),
617 but whether Trio activation of Rho ultimately acts through these PLCs to produce DAG is not
618 clear. One approach to test if these other PLCs mediate Rho signaling would be to perform
619 genetic epistasis experiments. However, loss of Rho-1 causes lethality (Jantsch-Plunger et al.,
620 2000; McMullan and Nurrish, 2011) and loss of PLCε cause sterility defects (Yin et al., 2004),
621 limiting our ability to measure differences in egg laying. Alternatively, $G\alpha_q$ signaling through the
622 Rho-1 branch may be independent of PLCs and DAG production where exogenous PMA is
623 instead activating factors downstream of a parallel PLCβ pathway. While our rescue data are
624 consistent with PLCβ acting in neurons and Trio RhoGEF acting in muscles, we cannot rule out
625 a PLCβ function for DAG or IP_3 production in the vulval muscles. Imaging or biochemical
626 approaches documenting $G\alpha_q$-dependent changes in PIP_2 (Stauffer et al., 1998) and/or DAG
627 (Ohno et al., 2017; Tewson et al., 2012) *in vivo*, along with cell-specific rescue and knockout
628 experiments (LeBoeuf et al., 2020), should resolve whether the Rho-1 branch acts through PLCs
629 and/or inhibits DAG lipases to promote DAG levels.

630 Do phorbol esters like PMA stimulate *C. elegans* egg laying by acting as DAG mimetics?
631 Previous studies have shown that phorbol esters promote both synaptic vesicle and dense core
632 vesicle release from neurons and neurosecretory cells (Silinsky and Searl, 2003). DAG and
633 phorbol esters activate many effectors including mUNC-13 in the brain and Protein Kinase C
634 (PKC) in nearly all cells (Betz et al., 1998; Huang, 1989). In *C. elegans*, exogenous treatment
635 with phorbol esters causes growth inhibition, uncoordinated movement, and lethality which can
636 be suppressed by loss-of-function mutations in a single gene, *tpa-1*, which encodes nPKCδ/θ
637 (Tabuse and Miwa, 1983; Tabuse et al., 1989). Acute PMA treatment promotes hypersensitivity
638 to the paralytic effects of aldicarb (Sieburth et al., 2007). Double mutants of both PKC-1 and

639 UNC-13 (H17K) show increased resistance to phorbol esters compared to either mutant alone
640 suggesting that PMA acts in part through these effectors to regulate ACh release (Sieburth et
641 al., 2007; Silinsky and Searl, 2003). Our data show that animals lacking UNC-13 still lay eggs in
642 response to PMA. Mutant animals with defects in single PKC isoform encoding genes were
643 similarly responsive to PMA, with the notable exception of *pkc-1(nj1)* mutant animals. *pkc-1(nj1)*
644 results in a missense mutation and shows a significantly reduced PMA response compared to
645 two other putative null mutants. Such allele-specific differences among *pkc-1* alleles have been
646 observed previously in experiments studying PKC function in nose touch response, octanol and
647 high osmolarity avoidance (Hyde et al., 2011), regulation of AWC^{ON} glutamate release
648 (Ventimiglia and Bargmann, 2017), and in regulation of PKC by DAG or Ca^{2+} (Okochi et al.,
649 2005). The *nj1* allele may impart a dominant-negative effect, affecting the recruitment or function
650 of other PKC isoforms. For example, TPA-1 has been shown to function redundantly with PKC-
651 1 (also known as TTX-4), a nPKC-ε ortholog (Okochi et al., 2005). Studies have shown that
652 activated $G\alpha_q$ and accumulation of DAG recruit TPA-1 to compensate for the loss of PKC-1
653 (Hiroki and Iino, 2022). Egg-laying defects of *egl-19(n582)* L-type Ca^{2+} channel mutants are
654 enhanced when combined with *tpa-1(k530)* PKC null mutants (Waggoner et al., 1998),
655 suggesting TPA-1 may mediate some of the DAG and/or PMA response for egg laying. Future
656 work testing compound mutants disrupting UNC-13 and different PKC isoforms should reveal
657 whether PMA acts as a DAG mimetic in neurons and muscle cells to promote egg laying.

658 Besides the compensatory effect of various PKCs and UNC-13, this study does not rule
659 out other effectors as potential targets of DAG and/or PMA. *In vitro* studies show ROCK (Rho-
660 associated coiled-coil kinase) activation in PMA-induced apoptosis and macrophage
661 differentiation (Chang et al., 2006; Yang et al., 2017). ROCK has a predicted C1 domain that
662 mediates protein interaction with DAG and might bind and be similarly activated by PMA (Xiao
663 et al., 2009). In *C. elegans,* RHO-1 signals through LET-502/ROCK to phosphorylate non-

664 muscle myosin light chain (Shimizu et al., 2018). $G\alpha_q$ also promotes neurotransmitter release
665 via additional kinase targets including SEK-1 Mitogen-Activated Protein Kinase Kinase in the
666 p38 MAPK pathway and KSR-1 in the ERK MAPK pathway (Coleman et al., 2018; Hoyt et al.,
667 2017). KSR-1 is particularly interesting in that its N-terminus shares sequence similarly with C1
668 domains that might mediate regulation by DAG. Loss of KSR-1 and other ERK MAPK
669 components also suppress the loopy locomotion defects caused by gain-of-function mutations
670 in Rho-1 (Coleman et al., 2018). Taken together, our work is consistent with a model where
671 additional DAG-sensitive effectors act downstream of $G\alpha_q$, Trio, and Rho to promote muscle
672 excitability and /or contractility for egg laying.

673 Phorbol esters and locally produced DAG may promote egg laying via activation of distinct
674 effectors. Apart from activation of C1 domain containing effectors, emerging evidence indicates
675 Phospholipase C-dependent production of DAG directly modulates the gating of ion channels
676 for membrane excitability. For example, DAG activates several ion channels including canonical
677 transient receptor potential (TRP) cation channels (TRPC) (Hofmann et al., 1999) while also
678 inhibiting other ion channels including two-pore domain TASK potassium channels via an
679 unknown mechanism (Wilke et al., 2014). PIP_2 has also been shown to modulate some ion
680 channels like KCNQ directly (Suh et al., 2006), although DAG and PMA modulate *C. elegans*
681 KCNQ channels likely via the intermediate activation of protein kinases including PKC (Wei et
682 al., 2005). Thus, $G\alpha_q$ modulation of PIP_2 and DAG levels could directly or indirectly affect several
683 postsynaptic ion channels to shape electrical excitability. DAG is also precursor in the production
684 of several signaling lipids, including the endocannabinoid 2-arachidonoylglycerol (2-AG) which
685 has been shown to signal from dendrites in a retrograde manner through neuronal $G\alpha_o$-coupled
686 endocannabinoid receptors to inhibit neurotransmitter release (Hashimotodani et al., 2013;
687 Hashimotodani et al., 2005; Soltesz et al., 2015; Tanimura et al., 2010; Wettschureck et al.,
688 2006). In *C. elegans*, 2-AG activates the NPR-19 endocannabinoid receptor ortholog that

689 couples to $G\alpha_o$ to modulate serotonin transmission, pharyngeal, feeding, and locomotory
690 behaviors (Oakes et al., 2019; Oakes et al., 2017; Pastuhov et al., 2016). We have recently
691 shown that feedback of egg accumulation alters vulval muscle Ca^{2+} activity, which subsequently
692 signals to regulate bursts of Ca^{2+} transients in the HSNs that accompany the onset of the egg-
693 laying active state (Ravi et al., 2018a; Ravi et al., 2021). These results support a model where
694 stretch-dependent feedback of egg accumulation stimulates postsynaptic vulval muscle Ca^{2+}
695 signaling. This Ca^{2+} could then activate PLCs to generate DAG and 2-AG which signal to
696 modulate HSN activity, serotonin release, and egg laying. The genetic and experimental
697 accessibility of the *C. elegans* egg-laying circuit should allow us to determine if conserved G
698 proteins like $G\alpha_q$ act generally to drive neural circuit activity via changes in DAG, subsequent
699 activation of effectors, and retrograde messengers like 2-AG.

700 **Acknowledgements**

701 This work was funded by grants from the NIH (R01-NS086932) and NSF (IOS-1844657) to KMC.
702 PD is supported by AHA predoctoral fellowship Award (20PRE35210233). We thank Drs.
703 Kenneth Miller, Joshua Kaplan, and Thomas Boulin for sharing plasmids and strains. Some of
704 the strains used in this study were provided by the *C. elegans* Genetics Center, which is funded
705 by NIH Office of Research Infrastructure Programs (P40 OD010440). We thank Drs. Julia
706 Dallman, Laura Bianchi, and Athula Wikramanayake along with members of the Collins lab for
707 helpful discussions and feedback on the manuscript.

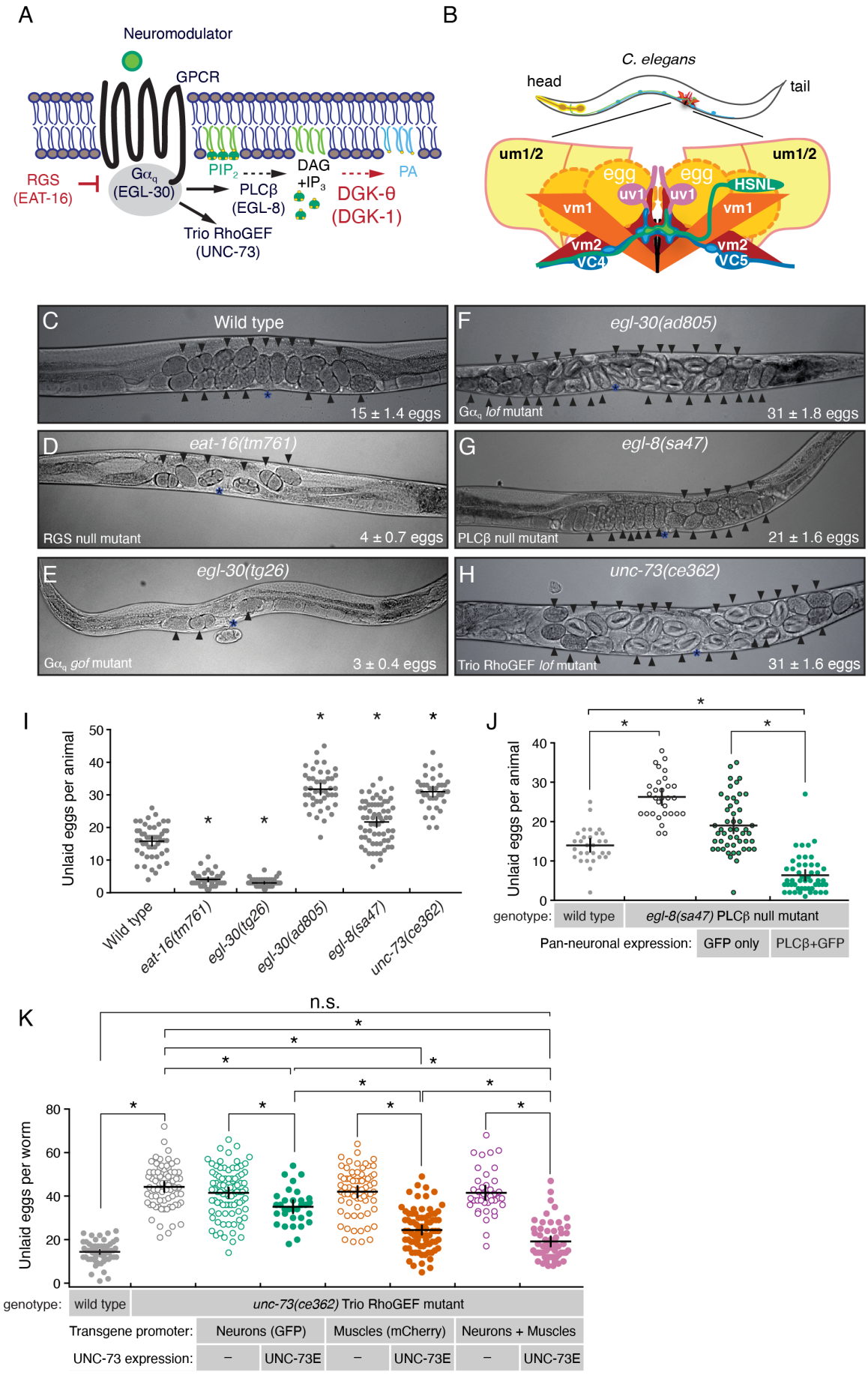
A
Neuromodulator
GPCR
RGS
(EAT-16)
Gαq
(EGL-30)
PIP2
PLCβ
(EGL-8)
DAG
+IP3
PA
DGK-θ
(DGK-1)
Trio RhoGEF
(UNC-73)
B
C. elegans
head
tail
um1/2
um1/2
egg
egg
uv1
uv1
HSNL
vm1
vm1
vm2
vm2
VC4
VC5
C
Wild type
15 ± 1.4 eggs
F
egl-30(ad805)
Gαq lof mutant
31 ± 1.8 eggs
D
eat-16(tm761)
RGS null mutant
4 ± 0.7 eggs
G
egl-8(sa47)
PLCβ null mutant
21 ± 1.6 eggs
E
egl-30(tg26)
Gαq gof mutant
3 ± 0.4 eggs
H
unc-73(ce362)
Trio RhoGEF lof mutant
31 ± 1.6 eggs
I
Unlaid eggs per animal
Wild type
eat-16(tm761)
egl-30(tg26)
egl-30(ad805)
egl-8(sa47)
unc-73(ce362)
J
Unlaid eggs per animal
genotype:
wild type
egl-8(sa47) PLCβ null mutant
Pan-neuronal expression:
GFP only
PLCβ+GFP
K
n.s.
Unlaid eggs per worm
genotype:
wild type
unc-73(ce362) Trio RhoGEF mutant
Transgene promoter:
Neurons (GFP)
Muscles (mCherry)
Neurons + Muscles
UNC-73 expression:
–
UNC-73E
–
UNC-73E
–
UNC-73E

708

709 **Figure 1: Trio RhoGEF acts in both neurons and muscles to regulate egg-laying behavior**
710 **(A)** Schematics of excitatory (black) and inhibitory (red) $G\alpha_q$ signaling pathway. *C. elegans* gene
711 names are beneath the protein they encode. **(B)** Cartoon of the *C. elegans* egg-laying circuit
712 from a lateral view. Only the left side of the bilaterally symmetric circuit is shown. HSNL,
713 Hermaphrodite Specific Neuron (left); VC4 and VC5 Ventral C neurons; vm1 and vm2 vulval
714 muscles, um1 and um2 uterine muscles; uv1 uterine-vulval neuroendocrine cells. **(C-H)** Bright
715 field images of worms of the indicated genotypes; arrowheads indicate accumulated eggs. Mean
716 number of accumulated eggs ± 95% confidence intervals is also indicated. Position of the vulva
717 is shown with an asterisk (*). **(I)** Scatterplot of egg accumulation in wild-type, *eat-16(tm761)*, *egl-*
718 *30(tg26)*, *egl-30(ad805), egl-8(sa47), and unc-73(ce362)* mutant animals. Line indicates mean
719 eggs ± 95% confidence intervals. Asterisks indicate p ≤0.0001 (One way ANOVA with
720 Bonferroni's correction; wild type (n=49); *eat-16(tm761)* (n=36); *egl-30(tg26)* (n=47); *egl-*
721 *30(ad805)* (n=44); *egl-8(sa47)* (n=65); *unc-73(ce362)* (n=38). **(J)** Transgenic rescue of *egl-8*
722 PLCβ egg-laying defects. Scatterplot of egg accumulation in transgenic animals expressing GFP
723 only or EGL-8/PLCβ fused to GFP expressed from the *rgs-1* promoter in *egl-8(sa47)* mutants
724 (n=50) compared to wild-type (n=30) and *egl-8(sa47)* mutant animals (n=30). Bar indicates mean
725 eggs ±95% confidence intervals. Asterisks indicate p≤0.0001 (One-way ANOVA with
726 Bonferroni's correction) **(K)** Transgenic rescue of *unc-73* Trio RhoGEF egg-laying defects.
727 Scatterplot of egg accumulation in wild-type (n=60), *unc-73(ce362)* mutants (n=72), and
728 transgenic animals expressing a fluorescent protein with or without Trio/UNC-73E in neurons
729 from the *rab-3* promoter (n≥32) or in muscles from the *myo-3* promoter (n≥69), or in both neurons
730 and muscles (n≥41) in *unc-73(ce362)* mutants. Horizontal line indicates mean accumulated eggs
731 ±95% confidence intervals. Asterisks indicate p≤0.0145; n.s.= not significant (p>0.05; One-way
732 ANOVA with Bonferroni's correction for multiple comparisons).
733

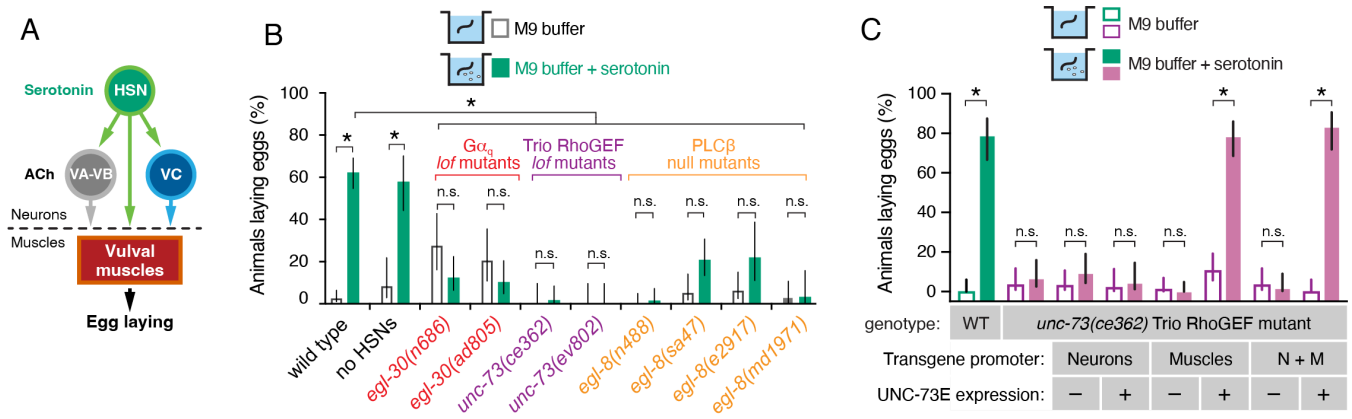

Figure 2: Serotonin signals through Gα$_q$, Trio, and PLCβ to promote egg laying.

(A) Model of serotonergic and acetylcholine (ACh) signaling in the egg-laying circuit. **(B)** Bar plots showing the percentage of animals laying eggs in M9 buffer alone (grey) or M9 +18.5 mM serotonin (green) after 1 hr. Bar indicates mean percent ±95% confidence intervals. Asterisks indicate p<0.0007; n.s.= not significant (p>0.05, Fisher's exact test with Bonferroni's correction for multiple comparisons; n>30 animals for each genotype and condition). **(C)** Bar plot showing percent of animals laying eggs in M9 buffer or M9 +18.5 mM serotonin in wild-type or Trio RhoGEF mutant animals expressing nothing or Trio/UNC-73E in neurons, muscles, or both. Bar indicates mean percent ±95% confidence intervals. Asterisks indicate p<0.0007; n.s.= not significant (p>0.05, Fisher's exact test with Bonferroni's correction for multiple comparisons; n>30 animals).

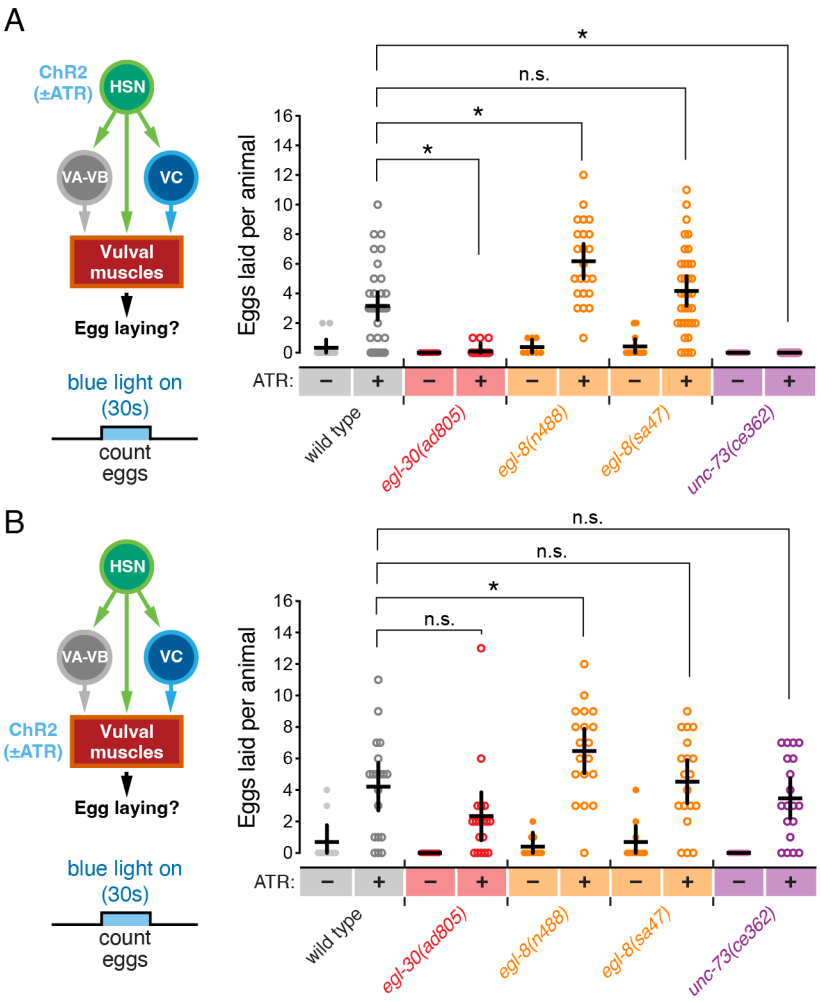

Figure 3: Optogenetic stimulation of the HSNs or vulval muscles reveals distinct cellular specificity of Gα_q effectors for egg laying. (A) On left, cartoon of the egg-laying circuit and experiment showing blue light activation of HSN for 30 seconds. On right, scatterplot showing eggs laid per worm in presence (+) or absence (-) of all-*trans* retinal (ATR) cofactor during the blue light activation of ChR2 expressed in HSNs of wild-type (grey), *egl-30(ad805)* Gα_q strong loss-of-function mutants (red), *egl-8(n488) and egl-8(sa47)* PLCβ mutants (orange), and *unc-73(ce362)* Trio mutant (purple) animals. Line indicates mean eggs laid ±95% confidence intervals. Asterisks indicate p<0.0001; n.s.= not significant (p>0.05, One-way ANOVA with Bonferroni's correction for multiple comparisons; n>10). **(B)** On the left, cartoon of the egg-laying circuit and experiment showing blue light activation of vulval muscles for 30 seconds(left). On

757 the right, scatter plots of eggs laid per worm in presence (+) or absence (-) of ATR during blue
758 light activation of ChR2 expressed in the vulval muscles of wild type, *egl-30(ad805)* $G\alpha_q$ strong
759 loss-of-function mutants (red), *egl-8(n488) and egl-8(sa47)* PLCβ mutants (orange), and *unc-*
760 *73(ce362)* Trio mutant (purple) animals. Line indicates mean eggs laid ±95% confidence
761 intervals. Asterisk indicates p≤0.0255; n.s.=not significant, p>0.05 (One-way ANOVA with
762 Bonferroni's correction for multiple comparisons; n>10).
763

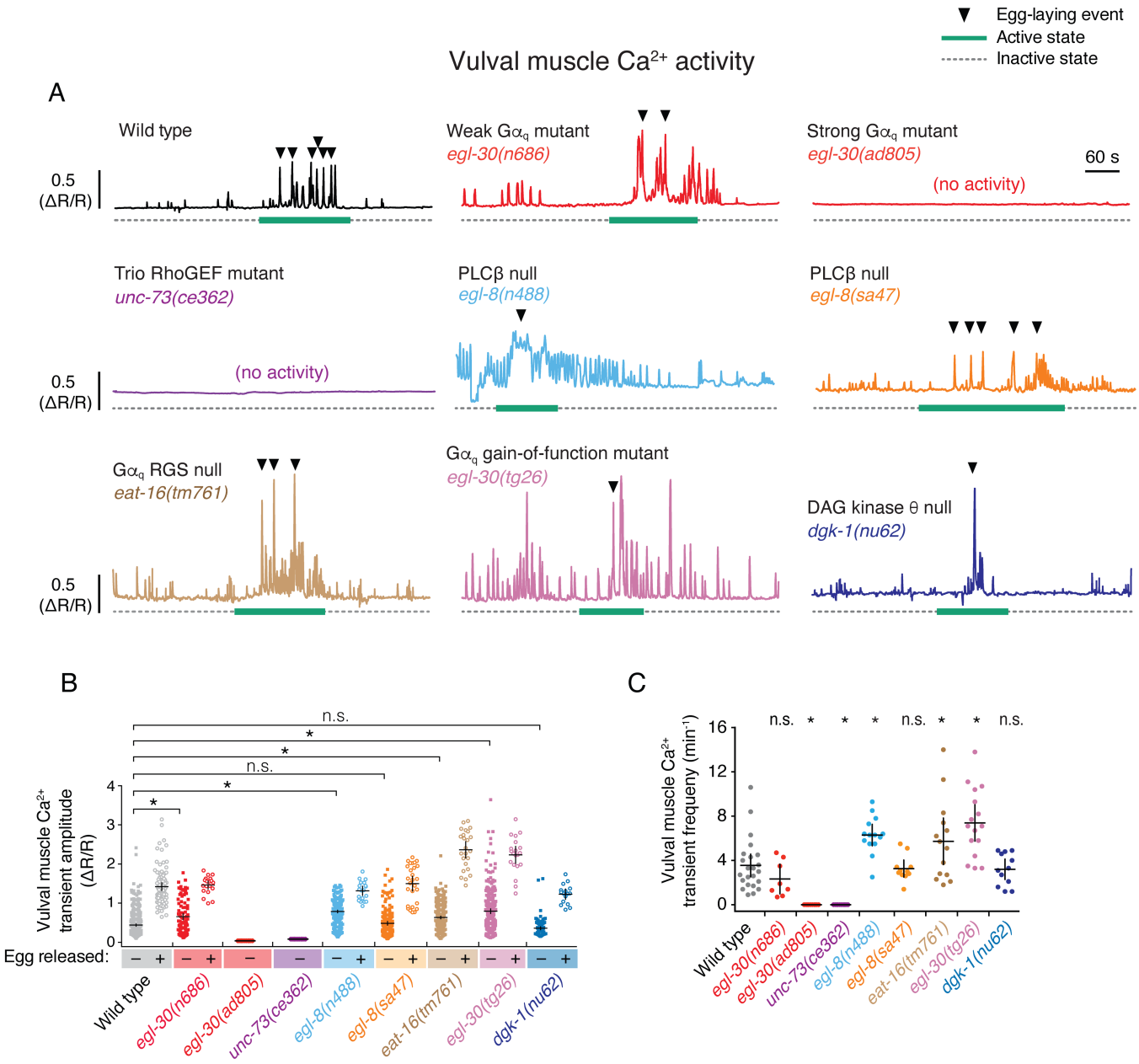

764 **Figure 4: $G\alpha_q$ and Trio signaling promotes vulval muscle activity. (A)** Representative
765 GCaMP5::mCherry (ΔR/R) ratio traces showing vulval muscle Ca^{2+} activity in freely behaving
766 wild-type (black), *egl-30(n686)* $G\alpha_q$ weak loss-of-function mutant (red), *egl-30(ad805)* $G\alpha_q$
767 strong loss-of-function mutant (red), *unc-73(ce362)* Trio strong loss-of-function mutant (purple),
768 *egl-8(n488)* PLCβ null mutant (light blue), *egl-8(sa47)* PLCβ null mutant (orange), *eat-16(tm761)*
769 $G\alpha_q$ RGS protein null mutant (grey), *egl-30(tg26)* strong $G\alpha_q$ gain-of-function mutant (magenta),
770 and *dgk-1(nu62)* DAG Kinase null mutant (dark blue) animals during active (green solid bar) and
771 inactive (dotted grey line) egg-laying behavior states. Arrowheads indicate egg-laying events.
772 Vertical and horizontal scale bars show GCaMP5/mCherry fluorescence ratio (ΔR/R) and time,
773 respectively **(B)** Scatterplots of Ca^{2+} transient peak amplitudes for the indicated genotypes
774 during twitch (closed square) and egg-laying transients (open circles). Asterisks indicate
775 $p<0.0001$, n.s. indicates not significant ($p>0.05$, Kruskal Wallis test with Dunn's correction for
776 multiple comparisons). **(C)** Scatterplots of Ca^{2+} transient frequency for indicated genotypes. Line
777 indicates mean eggs laid ±95% confidence intervals; asterisks indicate $p\leq0.0340$; n.s. indicates
778 not significant ($p>0.05$, One-way ANOVA with Bonferroni's correction for multiple comparisons;
779 n>10 animals recorded per genotype).
780

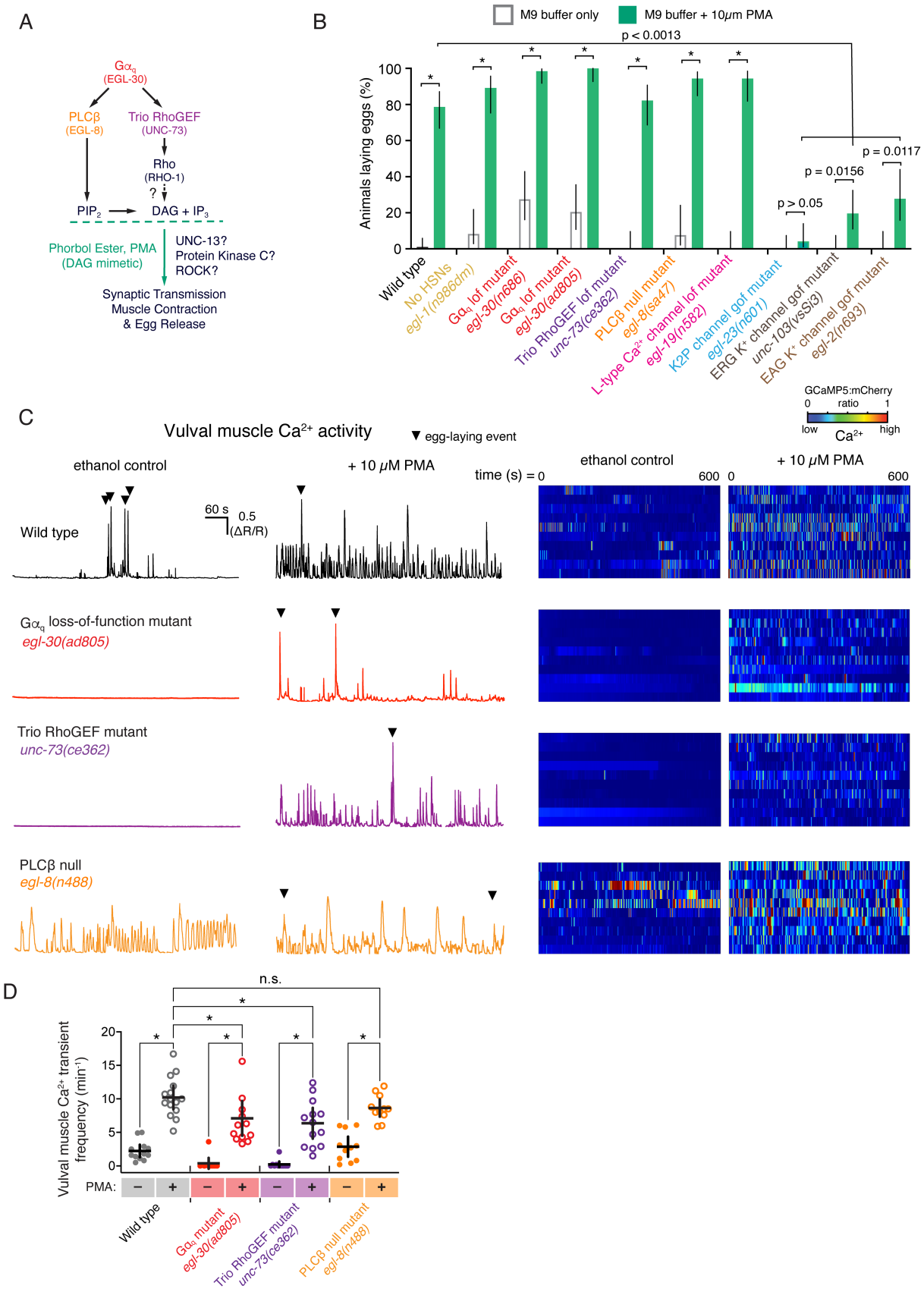
A
Gαq
(EGL-30)
PLCβ
(EGL-8)
Trio RhoGEF
(UNC-73)
Rho
(RHO-1)
?
PIP2
DAG + IP3
Phorbol Ester, PMA
(DAG mimetic)
UNC-13?
Protein Kinase C?
ROCK?
Synaptic Transmission
Muscle Contraction
& Egg Release
B
M9 buffer only
M9 buffer + 10μm PMA
p < 0.0013
p = 0.0117
p = 0.0156
p > 0.05
Animals laying eggs (%)
Wild type
No HSNs
egl-1(n986dm)
Gαq lof mutant
egl-30(n686)
Gαq lof mutant
egl-30(ad805)
Trio RhoGEF lof mutant
unc-73(ce362)
PLCβ null mutant
egl-8(sa47)
L-type Ca2+ channel lof mutant
egl-19(n582)
K2P channel gof mutant
egl-23(n601)
ERG K+ channel gof mutant
unc-103(vsSt3)
EAG K+ channel gof mutant
egl-2(n693)
C
Vulval muscle Ca2+ activity
egg-laying event
GCaMP5:mCherry
ratio
low
high
Ca2+
ethanol control
+ 10 μM PMA
time (s) = 0
600
60 s
0.5
(ΔR/R)
Wild type
Gαq loss-of-function mutant
egl-30(ad805)
Trio RhoGEF mutant
unc-73(ce362)
PLCβ null
egl-8(n488)
D
n.s.
Vulval muscle Ca2+ transient frequency (min-1)
PMA:
Wild type
Gαq mutant
egl-30(ad805)
Trio RhoGEF mutant
unc-73(ce362)
PLCβ null mutant
egl-8(n488)

781

782 **Figure 5: The DAG mimetic PMA rescues egg-laying circuit activity and behavior defects**
783 **of Gα_q signaling mutants**. **(A)** Diagrams showing working model of Gα_q and DAG signaling
784 pathway during egg-laying behavior. **(B)** Bar plots showing the percentage of animals showing
785 egg laying in M9 buffer (open grey bars) or M9 buffer +10 μM PMA (filled green bars). Error bars
786 indicate 95% confidence intervals for the proportion; asterisks indicate $p<0.0013$ (Fisher's exact
787 test with Bonferroni's correction for multiple comparisons; $n\geq30$ animals per genotype and
788 condition). **(C)** Left, representative GCaMP5::mCherry (ΔR/R) ratio traces showing vulval muscle
789 Ca^{2+} activity in wild-type or the indicated Gα_q signaling mutant animals in the absence or
790 presence of 10 μM PMA. Arrowheads indicate egg-laying events. Vertical and horizontal scale
791 bars show GCaMP5/mCherry fluorescence ratio (ΔR/R) and time, respectively. Right, heat map
792 showing intensity modulated color spectrum of GCaMP5::mCherry (ΔR/R) ratio of vulval muscle
793 Ca^{2+} activity ranging from blue (low Ca^{2+}) to red (high Ca^{2+}). Rows indicate ratio changes in each
794 of 10 animals. **(D)** Scatterplots of Ca^{2+} transient frequency in the absence (-) and presence (+)
795 of 10 μM PMA for the indicated genotypes. Lines indicate mean eggs laid ±95% confidence
796 intervals; asterisk indicates $p\leq0.0275$; n.s.= not significant ($p>0.05$, One-way ANOVA with
797 Bonferroni's correction for multiple comparisons; $n\geq10$ animals per genotype and condition).
798
799

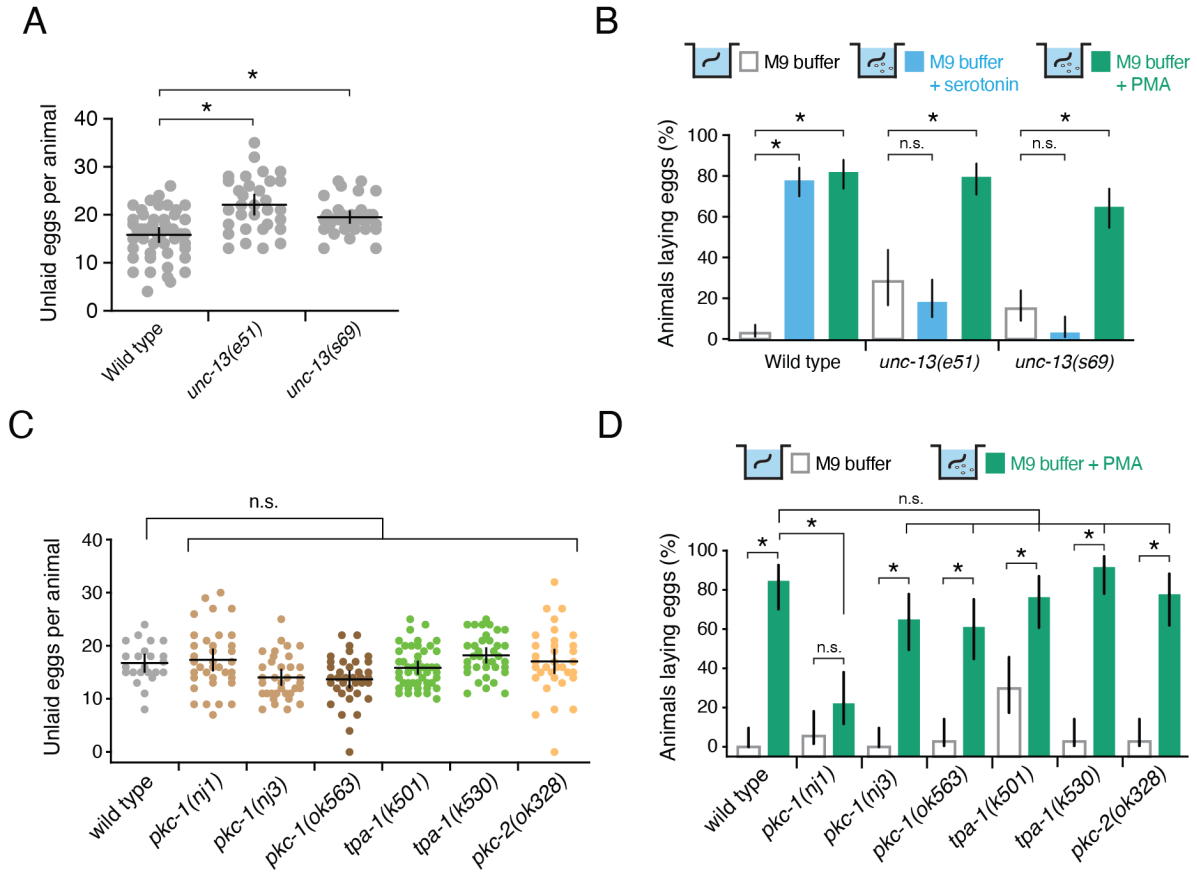

Figure 6: DAG promotes egg laying independent of UNC-13 or Protein Kinase C. (A) Scatterplot of egg accumulation in wild-type, *unc-13(e51)* loss-of-function mutant, and *unc-13(s69)* null mutant animals. Lines indicate mean eggs laid ±95% confidence intervals. Asterisk indicates p≤0.0021 (One-way ANOVA with Bonferroni's correction for multiple comparisons; n≥36 per genotype). (**B)** Bar plots showing the percentage of wild-type, *unc-13(e51),* or *unc-13(s69)* mutant animals laying eggs in M9 buffer (grey open boxes), 18.5 mM serotonin (filled blue boxes), or 10 μM PMA (filled green boxes). Asterisks indicate p<0.0006; n.s. = not significant (p>0.05, Fisher's exact test with Bonferroni's correction for multiple comparisons; n≥36 animals per genotype and condition). **(C)** Scatterplot of egg accumulation in wild-type (n=24) and the indicated Protein Kinase C mutant animals (n≥35 per genotype). Line indicates mean eggs accumulated ±95% confidence intervals. n.s.= not significant (p>0.05, One-way

813 ANOVA with Bonferroni's correction for multiple comparisons. **(D)** Bar plots showing the
814 percentage of wild-type and Protein Kinase C mutant animals showing egg laying in M9 buffer
815 (open bars) or 10 μM PMA (filled green bars). Bar indicates mean eggs ±95% confidence
816 intervals for the proportion. Asterisks indicate $p<0.0007$; n.s.= not significant ($p>0.05$, Fisher's
817 exact test with Bonferroni correction for multiple comparisons; $n\geq35$ animals per genotype and
818 condition).
819

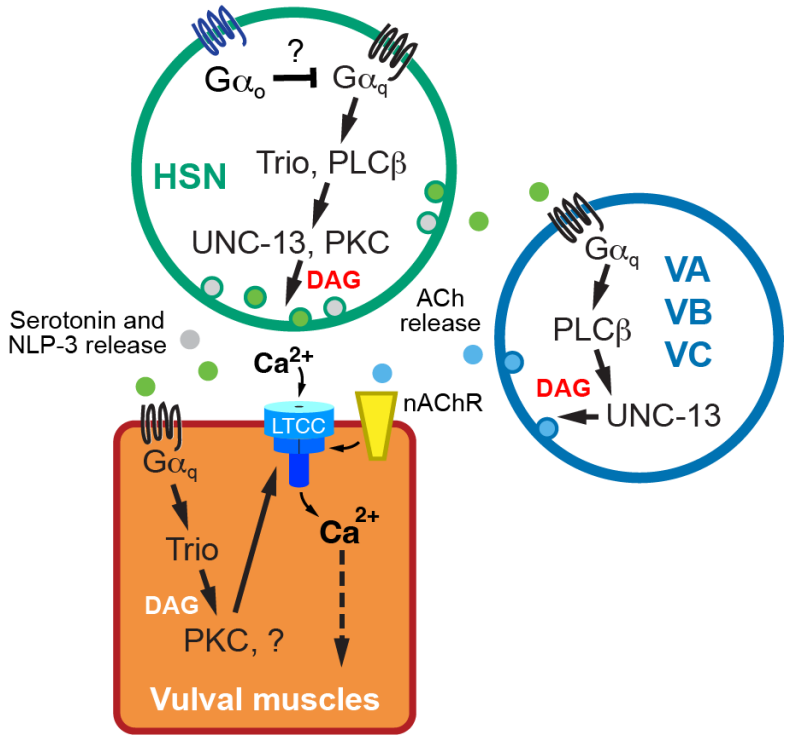

820

821 **Figure 7: Working model of Gα$_q$ signaling in the egg-laying circuit.** See text for details.

822 **Movie 1: GCaMP5:mCherry fluorescence ratio in the vulval muscles of wild-type animals**
823 **in the absence or presence of 10 μM DAG analogue, PMA.** Blue indicates low $Ca^{2+,}$ and red
824 indicates elevated Ca^{2+}.

825

826 **Movie 2: GCaMP5:mCherry fluorescence ratio in the vulval muscles of strong loss of**
827 **function $G\alpha_q$ mutant, *egl-30(ad805),* animals in the absence or presence of 10 μM DAG**
828 **analogue, PMA.** Blue indicates low $Ca^{2+,}$ and red indicates elevated Ca^{2+}.

829

830 **Movie 3: GCaMP5:mCherry fluorescence ratio in the vulval muscles of strong loss of**
831 **function Trio mutant, *unc-73(ce362)*, animals in the absence or presence of PMA.** Blue
832 indicates low $Ca^{2+,}$ and red indicates elevated Ca^{2}.

833

834 **Table 1: *C. elegans* strains used in this study**

Strains	Genotype	Feature	Source
N2	Wild type	Bristol wild-type strain	(Brenner, 1974)
MT1434	*egl-30(n686) I*	$G\alpha_q$ loss-of-function mutant, Egg-laying defective	(Trent et al., 1983)
DA823	*egl-30(ad805) I*	$G\alpha_q$ strong loss-of-function mutant, Egg-laying defective	(Brundage et al., 1996; Mendel et al., 1995)
KG1278	*unc-73(ce362) I*	Trio RhoGEF loss-of-function mutant, Egg-laying defective	(Williams et al., 2007)
KG1397	*unc-73(ev802) I*	Trio RhoGEF deletion mutant, Egg-laying defective	(Williams et al., 2007)
JT47	*egl-8(sa47) V*	PLCβ null, Egg-laying defective	(Thomas, 1990)
MT1083	*egl-8(n488) V*	PLCβ null, Egg-laying defective	(Trent et al., 1983)
CB6614	*egl-8(e2917) V*	PLCβ null, Egg-laying defective	(Yook and Hodgkin, 2007)
RM1221	*egl-8(md1971) V*	PLCβ null, Egg-laying defective	(Miller et al., 1999)

JIP2081	*egl-23(bln360[n601]) IV; lin-15AB(n765) vsIs164 lite-1(ce314) X*	Egg-laying defective	(Thomas, 1990) and this study
MT1212	*egl-19(n582) IV*	Egg-laying defective	(Trent et al., 1983)
MT1444	*egl-2(n693) V*	Egg-laying defective	(Trent et al., 1983)
LX1226	*eat-16(tm761) I*	$G\alpha_q$ RGS null, Hyperactive egg laying	(Porter and Koelle, 2010)
CG21	*egl-30(tg26) I; him-5(e1490) V*	$G\alpha_q$ gain-of-function mutant, Hyperactive egg-laying	(Garcia et al., 2001)
LX1832	*lite-1(ce314) lin-15(n765ts) X*	Used for transgenic line creation	(Gürel et al., 2012)
LX1286	*egl-8(sa47) I; lin-15(n765ts) X*	PLCβ null mutant, Egg-laying defective; multi-vulva	This study
LX1674	*egl-8(sa47) I; lin-15(n765ts) X; vsEx679*	PLCβ null, Egg-laying defective; non-Muv, expresses GFP in neurons from *rgs-1* promoter	This study
LX1675	*egl-8(sa47) I; lin-15(n765ts) X; vsEx680*	PLCβ null, Egg laying defective; non-Muv, expresses PLCβ and GFP in neurons from *rgs-1* promoter	This study
MIA26	*egl-1(n986dm) V*	Lacks HSNs	(Ravi et al., 2018a)
LX1918	*vsIs164 lite-1(ce314) lin-15(n765ts) X*	Expresses GCaMP5 and mCherry in the vulval muscles	(Li et al., 2013)
MIA109	*egl-8(sa47) V; vsIs164 lite-1(ce314), lin-15(n765ts) X*	Expresses GCaMP5 and mCherry in the vulval muscles of *egl-8(sa47)* mutant	This study
MIA139	*egl-30(n686) I; vsIs164 lite-1(ce314) lin-15(n765ts) X*	Expresses GCaMP5 and mCherry in the vulval muscles of *egl-30(n686*)	This study
MIA140	*egl-30(ad805) I; vsIs164 lite-1(ce314), lin-15(n765ts) X*	Expresses GCaMP5 and mCherry in the vulval muscles of *egl-30(ad805)*	This study
MIA141	*unc-73(ce362) I; vsIs164, lite-1(ce314) lin-15(n765ts) X*	Expresses GCaMP5 and mCherry in the vulval muscles of *unc-73(ce362)*	This study
MIA286	*egl-30(tg26) I; vsIs164, lite-1(ce314) lin-15(n765ts) X*	Expresses GCaMP5 and mCherry in the vulval muscles of *egl-30(tg26)*	This study
MIA287	*eat-16(tm761) I; vsIs164 lite-1(ce314) lin-15(n765ts) X*	Expresses GCaMP5 and mCherry in the vulval muscles of *eat-16(tm761)*	This study

MIA288	*egl-8(n488) V; vsIs164 lite-1 (ce314) lin-15(n765ts) X*	Expresses GCaMP5 and mCherry in the vulval muscles of *egl-8(n488)*	This study
MIA296	*dgk-1(nu62) lite-1(ce314) lin-15(n765ts) X*	Expresses GCaMP5 and mCherry in the vulval muscles of *dgk-1(nu62)*	This study
MIA372	*unc-73(ce362) I; keyEx64*	Expresses GFP in the neurons and mCherry in the muscles of *unc-73(ce362)*	This study
MIA373	*unc-73(ce362) I; keyEx65*	Expresses GFP and Trio RhoGEF-E cDNA in the neurons, and mCherry and Trio RhoGEF-E cDNA in the muscles of *unc-73(ce362)*	This study
MIA374	*unc-73(ce362) I; keyEx66*	Expresses GFP in neurons	This study
MIA375	*unc-73(ce362) I; keyEx67*	Expresses GFP and Trio RhoGEF-E cDNA in neurons	This study
MIA376	*unc-73(ce362) I; keyEx68*	Expresses mCherry in muscles	This study
MIA377	*unc-73(ce362) I; keyEx69*	Expresses mCherry and Trio RhoGEF-E cDNA in muscles	This study
LX1836	*wzIs30 IV; lite-1(ce314) lin-15(n765ts) X*	Expresses Channelrhodopsin-2 (ChR2) in HSNs from the *egl-6* promoter	(Collins et al., 2016)
MIA229	*keyIs48; lite-1(ce314) lin-15(n765ts) X*	Expresses ChR2 in vulval muscles from the *ceh-24* promoter	(Kopchock et al., 2021)
MIA300	*egl-30(ad805) I; wzIs30 IV; lite-1(ce314) X*	Expresses ChR2 in HSN of *egl-30(ad805)* mutant	This study
MIA301	*egl-30(ad805) I; keyIs48; lite-1(ce314) X*	Expresses ChR2 in vulval muscles of *egl-30(ad805)* mutant	This study
MIA304	*wzIs30 IV; egl-8(n488) V; lite-1(ce314) X*	Expresses ChR2 in HSNs of *egl-8(n488)* mutant	This study
MIA305	*egl-8(n488) V; keyIs48; lite-1(ce314) X*	Expresses ChR2 in vulval muscles of *egl-8(n488)* mutant	This study
MIA308	*wzIs30 IV; egl-8(sa47) V; lite-1(ce314) X*	Express ChR2 in HSNs of *egl-8(sa47)* mutant	This study
MIA309	*egl-8(sa47) V; keyIs48; lite-1(ce314) X*	Expresses ChR2 in vulval muscles of *egl-8(sa47)* mutant	This study

MIA247	*unc-73(ce362) I; wzIs30 IV; lite-1(ce314) X*	Expresses ChR2 in HSN of *unc-73(ce362)* mutant	This study
MIA248	*unc-73(ce362) I; keyIs48; lite-1(ce314) X*	Expresses ChR2 in vulval muscles of *unc-73(ce362)* mutant	This study
LX1615	*vsSi3[Punc-103e::unc-103(e1597dm)-GFP::unc-103, cb-unc-119(+)] II*	Expresses gain-of-function A331T UNC-103 ERG channel in the vulval muscles from the *unc-103e* promoter	This study
MT7929	*unc-13(e51) I*	UNC-13 loss-of-function	(Brenner, 1974)
EG9631	*unc-13(s69) I*	UNC-13 null	(Rose and Baillie, 1980)
IK105	*pkc-1(nj1) V*	nPKCε null	(Okochi et al., 2005)
IK130	*pkc-1(nj3) V*	nPKCε null	(Okochi et al., 2005)
RB781	*pkc-1(ok563) V*	nPKCε null	(Consortium, 2012)
VC127	*pkc-2(ok328) X*	cPKCα/β null	(Consortium, 2012)
MJ500	*tpa-1(k501) IV*	nPKCδ/θ null	(Tabuse et al., 1989)
MJ563	*tpa-1(k530) IV*	nPKCδ/θ null	(Tabuse et al., 1989)

838 **Table 2: Oligonucleotide sequences used in this study**

Oligo Name	Sequence (5'>3')	Use
lite-1(ce314)-fwd	ACGGGAGACGAAGAGCTAAAT AGG	Genotyping of *lite-1(ce314)*
lite-1(ce314)-rev	CTAAGTTGCCGGTTGCCTTAG AAC	Genotyping of *lite-1(ce314)*
egl-30(n686)-F	GCCAACCGAGCAGGACATTCTG CG	Genotyping of *egl-30(n686)*
eg-30(n686)-R	CGGGAAAGTAGTCAGCGAGAT GCG	Genotyping of *egl-30(n686)*
egl-30(ad805)-F	GCCAGGGCTGTCCCATTACGG	Genotyping of *egl-30(ad805)*
egl-30(ad805)-R	TCGGAAAGCGCCACCAGGAAC	Genotyping of *egl-30(ad805)*
egl-8-cDNA-fwd	CTTGGCTAGCGTAGAAAAAATG GCAAAGGAGTTCCAGTTC	For amplification of *egl-8* coding sequences
egl-8-cDNA-rev	CGCCCATGGTTATCAAACGACA GAAGTCGGTTGAGC	For amplification of *egl-8* coding sequences
egl-8-Cterm-NotI-fwd	GTGGGTACTCCACTGGGGGTG CGGCCGCTGGAGGTCCTTCGA CACCGGT	Quick change mutagenesis of *egl-8* cDNA to insert in-frame NotI enzyme for GFP insertion
egl-8-Cterm-NotI-rev	ACCGGTGTCGAAGGACCTCCA GCGGCCGCACCC CCAGTGGAGTACCCAC	Quick-change mutagenesis of *egl-8* cDNA to insert in-frame NotI enzyme for GFP insertion
NotI-GFP-FWD	GGTGCGGCCGCTGGAAGTAAA GGAGAAGAACTTTTC	For amplification of GFP with flanking, in-frame NotI enzyme sites for insertion into *egl-8* cDNA
NotI-GFP-REV	TCCAGCGGCCGCTCCTTTGTAT AGTTCATCCATGCC	For amplification of GFP with flanking, in-frame NotI enzyme sites for insertion into *egl-8* cDNA
RE-GFP-FWD-new	GCGTCTAGAACCGGTGCTAGC GTAGAAAAAATGGTCAGTAAAG GAGAAGAACTTTTC	For amplification of sequences encoding GFP for cloning into pGP3 *rgs-1* promoter containing plasmid
RE-GFP-REV	TACGAATTCGGTACCTCAGATT TATTTGTATAGTTCATCCATG	For amplification of sequences encoding GFP for cloning into pGP3 *rgs-1* promoter containing plasmid
unc-103(gf)-QC-fwd	CTC GGT TCT TTG ATG TAC ACC TCT GTG TTC GGT AAT G	For QuickChange mutagenesis of *unc-103* coding sequences to insert the A331T mutation present in the *e1597gf* mutant.
unc-103(gf)-QC-rev	CAT TAC CGA ACA CAG AGG TGT ACA TCA AAG AAC CGA G	For QuickChange mutagenesis of *unc-103* coding sequences to insert the A331T mutation present in the *e1597gf* mutant.

839

840 **Table 3: Serotonin-induced egg laying in *egl-8* PLCβ mutants**

841

		60 min		**90 min**		
Genotype	N	Average eggs laid in 18.5 mM serotonin	Std. Deviation	Average eggs laid in 18.5 mM serotonin	Std. Deviation	**P value (Paired t test)**
wild type (N2)	64	1.8	1.7	5.8	4.5	<0.0001
egl-8(e2917)	32	0.2	0.6	1.4	2.5	0.0091
egl-8(n488)	32	0.0	0.2	0.1	0.3	0.0831
egl-8(md1971)	32	0.3	0.8	1.3	2.1	0.0075
egl-8(sa47)	32	0.8	1.4	2.5	2.5	0.0002

842 **References:**

843 Akerboom, J., Carreras Calderon, N., Tian, L., Wabnig, S., Prigge, M., Tolo, J., Gordus, A.,
844 Orger, M.B., Severi, K.E., Macklin, J.J., *et al.* (2013). Genetically encoded calcium
845 indicators for multi-color neural activity imaging and combination with optogenetics. Front
846 Mol Neurosci *6*, 2.

847 Ananthanarayanan, B., Stahelin, R.V., Digman, M.A., and Cho, W. (2003). Activation
848 mechanisms of conventional protein kinase C isoforms are determined by the ligand
849 affinity and conformational flexibility of their C1 domains. J Biol Chem *278*, 46886-46894.

850 Avery, L., Bargmann, C.I., and Horvitz, H.R. (1993). The Caenorhabditis elegans unc-31 gene
851 affects multiple nervous system-controlled functions. Genetics *134*, 455-464.

852 Banerjee, N., Bhattacharya, R., Gorczyca, M., Collins, K.M., and Francis, M.M. (2017). Local
853 neuropeptide signaling modulates serotonergic transmission to shape the temporal
854 organization of C. elegans egg-laying behavior. PLoS Genet *13*, e1006697.

855 Bany, I.A., Dong, M.Q., and Koelle, M.R. (2003). Genetic and cellular basis for acetylcholine
856 inhibition of Caenorhabditis elegans egg-laying behavior. J Neurosci *23*, 8060-8069.

857 Bastiani, C.A., Gharib, S., Simon, M.I., and Sternberg, P.W. (2003). Caenorhabditis elegans
858 Galphaq regulates egg-laying behavior via a PLCbeta-independent and serotonin-
859 dependent signaling pathway and likely functions both in the nervous system and in
860 muscle. Genetics *165*, 1805-1822.

861 Ben Soussia, I., El Mouridi, S., Kang, D., Leclercq-Blondel, A., Khoubza, L., Tardy, P., Zariohi,
862 N., Gendrel, M., Lesage, F., Kim, E.J., *et al.* (2019). Mutation of a single residue promotes
863 gating of vertebrate and invertebrate two-pore domain potassium channels. Nat Commun
864 *10*, 787.

865 Berridge, M.J., Lipp, P., and Bootman, M.D. (2000). The versatility and universality of calcium
866 signalling. Nat Rev Mol Cell Biol *1*, 11-21.

867 Betke, K.M., Wells, C.A., and Hamm, H.E. (2012). GPCR mediated regulation of synaptic
868 transmission. Prog Neurobiol *96*, 304-321.
869 Betz, A., Ashery, U., Rickmann, M., Augustin, I., Neher, E., Sudhof, T.C., Rettig, J., and Brose,
870 N. (1998). Munc13-1 is a presynaptic phorbol ester receptor that enhances
871 neurotransmitter release. Neuron *21*, 123-136.
872 Brenner, S. (1974). The genetics of Caenorhabditis elegans. Genetics *77*, 71-94.
873 Brewer, J.C., Olson, A.C., Collins, K.M., and Koelle, M.R. (2019). Serotonin and neuropeptides
874 are both released by the HSN command neuron to initiate Caenorhabditis elegans egg
875 laying. PLoS Genet *15*, e1007896.
876 Brose, N., and Rosenmund, C. (2002). Move over protein kinase C, you've got company:
877 alternative cellular effectors of diacylglycerol and phorbol esters. J Cell Sci *115*, 4399-
878 4411.
879 Brundage, L., Avery, L., Katz, A., Kim, U.J., Mendel, J.E., Sternberg, P.W., and Simon, M.I.
880 (1996). Mutations in a C. elegans Gqalpha gene disrupt movement, egg laying, and
881 viability. Neuron *16*, 999-1009.
882 Chang, Y.C., Lee, H.H., Chen, Y.J., Bokoch, G.M., and Chang, Z.F. (2006). Contribution of
883 guanine exchange factor H1 in phorbol ester-induced apoptosis. Cell Death Differ *13*,
884 2023-2032.
885 Chase, D.L., and Koelle, M.R. (2004). Genetic analysis of RGS protein function in
886 Caenorhabditis elegans. Methods Enzymol *389*, 305-320.
887 Chhatriwala, M.K., Betts, L., Worthylake, D.K., and Sondek, J. (2007). The DH and PH domains
888 of Trio coordinately engage Rho GTPases for their efficient activation. J Mol Biol *368*,
889 1307-1320.
890 Coleman, B., Topalidou, I., and Ailion, M. (2018). Modulation of Gq-Rho Signaling by the ERK
891 MAPK Pathway Controls Locomotion in Caenorhabditis elegans. Genetics *209*, 523-535.

892 Collins, K.M., Bode, A., Fernandez, R.W., Tanis, J.E., Brewer, J.C., Creamer, M.S., and Koelle,
893 M.R. (2016). Activity of the C. elegans egg-laying behavior circuit is controlled by
894 competing activation and feedback inhibition. Elife *5*.
895 Collins, K.M., and Koelle, M.R. (2013). Postsynaptic ERG potassium channels limit muscle
896 excitability to allow distinct egg-laying behavior states in Caenorhabditis elegans. J
897 Neurosci *33*, 761-775.
898 Consortium, C.e.D.M. (2012). large-scale screening for targeted knockouts in the
899 Caenorhabditis elegans genome. G3 (Bethesda) *2*, 1415-1425.
900 Cook, S.J., Jarrell, T.A., Brittin, C.A., Wang, Y., Bloniarz, A.E., Yakovlev, M.A., Nguyen, K.C.Q.,
901 Tang, L.T., Bayer, E.A., Duerr, J.S.*, et al.* (2019). Whole-animal connectomes of both
902 Caenorhabditis elegans sexes. Nature *571*, 63-71.
903 Dempsey, C.M., Mackenzie, S.M., Gargus, A., Blanco, G., and Sze, J.Y. (2005). Serotonin
904 (5HT), fluoxetine, imipramine and dopamine target distinct 5HT receptor signaling to
905 modulate Caenorhabditis elegans egg-laying behavior. Genetics *169*, 1425-1436.
906 Doi, M., and Iwasaki, K. (2002). Regulation of retrograde signaling at neuromuscular junctions
907 by the novel C2 domain protein AEX-1. Neuron *33*, 249-259.
908 Dong, M.Q., Chase, D., Patikoglou, G.A., and Koelle, M.R. (2000). Multiple RGS proteins alter
909 neural G protein signaling to allow C. elegans to rapidly change behavior when fed. Genes
910 Dev *14*, 2003-2014.
911 Edwards, M.R., Johnson, J.R., Rankin, K., Jenkins, R.E., Maguire, C., Morgan, A., Burgoyne,
912 R.D., and Barclay, J.W. (2012). PKC-2 phosphorylation of UNC-18 Ser322 in AFD neurons
913 regulates temperature dependency of locomotion. J Neurosci *32*, 7042-7051.
914 Emtage, L., Aziz-Zaman, S., Padovan-Merhar, O., Horvitz, H.R., Fang-Yen, C., and Ringstad,
915 N. (2012). IRK-1 potassium channels mediate peptidergic inhibition of Caenorhabditis
916 elegans serotonin neurons via a G(o) signaling pathway. J Neurosci *32*, 16285-16295.

917 Fernandez, R.W., Wei, K., Wang, E.Y., Mikalauskaite, D., Olson, A., Pepper, J., Christie, N.,
918 Kim, S., Weissenborn, S., Sarov, M.*, et al.* (2020). Cellular Expression and Functional
919 Roles of All 26 Neurotransmitter GPCRs in the C. elegans Egg-Laying Circuit. J Neurosci
920 *40*, 7475-7488.
921 Frokjaer-Jensen, C., Davis, M.W., Hopkins, C.E., Newman, B.J., Thummel, J.M., Olesen, S.P.,
922 Grunnet, M., and Jorgensen, E.M. (2008). Single-copy insertion of transgenes in
923 Caenorhabditis elegans. Nat Genet *40*, 1375-1383.
924 Gao, S., and Zhen, M. (2011). Action potentials drive body wall muscle contractions in
925 Caenorhabditis elegans. Proc Natl Acad Sci U S A *108*, 2557-2562.
926 Garcia, L.R., Mehta, P., and Sternberg, P.W. (2001). Regulation of distinct muscle behaviors
927 controls the C. elegans male's copulatory spicules during mating. Cell *107*, 777-788.
928 Geppetti, P., Veldhuis, N.A., Lieu, T., and Bunnett, N.W. (2015). G Protein-Coupled Receptors:
929 Dynamic Machines for Signaling Pain and Itch. Neuron *88*, 635-649.
930 Gürel, G., Gustafson, M.A., Pepper, J.S., Horvitz, H.R., and Koelle, M.R. (2012). Receptors and
931 other signaling proteins required for serotonin control of locomotion in Caenorhabditis
932 elegans. Genetics *192*, 1359-1371.
933 Hajdu-Cronin, Y.M., Chen, W.J., Patikoglou, G., Koelle, M.R., and Sternberg, P.W. (1999).
934 Antagonism between G(o)alpha and G(q)alpha in Caenorhabditis elegans: the RGS
935 protein EAT-16 is necessary for G(o)alpha signaling and regulates G(q)alpha activity.
936 Genes Dev *13*, 1780-1793.
937 Hashimotodani, Y., Ohno-Shosaku, T., Tanimura, A., Kita, Y., Sano, Y., Shimizu, T., Di Marzo,
938 V., and Kano, M. (2013). Acute inhibition of diacylglycerol lipase blocks endocannabinoid-
939 mediated retrograde signalling: evidence for on-demand biosynthesis of 2-
940 arachidonoylglycerol. J Physiol *591*, 4765-4776.

941 Hashimotodani, Y., Ohno-Shosaku, T., Tsubokawa, H., Ogata, H., Emoto, K., Maejima, T.,
942 Araishi, K., Shin, H.S., and Kano, M. (2005). Phospholipase Cbeta serves as a
943 coincidence detector through its Ca2+ dependency for triggering retrograde
944 endocannabinoid signal. Neuron *45*, 257-268.
945 Hiley, E., McMullan, R., and Nurrish, S.J. (2006). The Galpha12-RGS RhoGEF-RhoA signalling
946 pathway regulates neurotransmitter release in C. elegans. Embo j *25*, 5884-5895.
947 Hiroki, S., and Iino, Y. (2022). The redundancy and diversity between two novel PKC isotypes
948 that regulate learning in Caenorhabditis elegans. Proc Natl Acad Sci U S A *119*.
949 Hofmann, T., Obukhov, A.G., Schaefer, M., Harteneck, C., Gudermann, T., and Schultz, G.
950 (1999). Direct activation of human TRPC6 and TRPC3 channels by diacylglycerol. Nature
951 *397*, 259-263.
952 Hoyt, J.M., Wilson, S.K., Kasa, M., Rise, J.S., Topalidou, I., and Ailion, M. (2017). The SEK-1
953 p38 MAP Kinase Pathway Modulates Gq Signaling in Caenorhabditis elegans. G3
954 (Bethesda) *7*, 2979-2989.
955 Hu, S., Pawson, T., and Steven, R.M. (2011). UNC-73/trio RhoGEF-2 activity modulates
956 Caenorhabditis elegans motility through changes in neurotransmitter signaling upstream
957 of the GSA-1/Galphas pathway. Genetics *189*, 137-151.
958 Huang, K.P. (1989). The mechanism of protein kinase C activation. Trends Neurosci *12*, 425-
959 432.
960 Hyde, R., Corkins, M.E., Somers, G.A., and Hart, A.C. (2011). PKC-1 acts with the ERK MAPK
961 signaling pathway to regulate Caenorhabditis elegans mechanosensory response. Genes
962 Brain Behav *10*, 286-298.
963 Jacob, T.C., and Kaplan, J.M. (2003). The EGL-21 carboxypeptidase E facilitates acetylcholine
964 release at Caenorhabditis elegans neuromuscular junctions. J Neurosci *23*, 2122-2130.

965 Jantsch-Plunger, V., Gönczy, P., Romano, A., Schnabel, H., Hamill, D., Schnabel, R., Hyman,
966 A.A., and Glotzer, M. (2000). CYK-4: A Rho family gtpase activating protein (GAP)
967 required for central spindle formation and cytokinesis. J Cell Biol *149*, 1391-1404.
968 Jose, A.M., and Koelle, M.R. (2005). Domains, amino acid residues, and new isoforms of
969 Caenorhabditis elegans diacylglycerol kinase 1 (DGK-1) important for terminating
970 diacylglycerol signaling in vivo. J Biol Chem *280*, 2730-2736.
971 Jospin, M., Jacquemond, V., Mariol, M.C., Segalat, L., and Allard, B. (2002). The L-type voltage-
972 dependent Ca2+ channel EGL-19 controls body wall muscle function in Caenorhabditis
973 elegans. J Cell Biol *159*, 337-348.
974 Kass, J., Jacob, T.C., Kim, P., and Kaplan, J.M. (2001). The EGL-3 proprotein convertase
975 regulates mechanosensory responses of Caenorhabditis elegans. J Neurosci *21*, 9265-
976 9272.
977 Kim, J., Poole, D.S., Waggoner, L.E., Kempf, A., Ramirez, D.S., Treschow, P.A., and Schafer,
978 W.R. (2001). Genes affecting the activity of nicotinic receptors involved in Caenorhabditis
979 elegans egg-laying behavior. Genetics *157*, 1599-1610.
980 Konig, B., DiNitto, P.A., and Blumberg, P.M. (1985). Stoichiometric binding of diacylglycerol to
981 the phorbol ester receptor. J Cell Biochem *29*, 37-44.
982 Kopchock, R.J. (2021). The Role of Acetylcholine Signaling in the C. elegans Egg-Laying Circuit.
983 In A&S - Biology (University of Miami).
984 Kopchock, R.J., 3rd, Ravi, B., Bode, A., and Collins, K.M. (2021). The sex-specific VC neurons
985 are mechanically activated motor neurons that facilitate serotonin-induced egg laying in C.
986 elegans. J Neurosci.
987 Kunitomo, H., Sato, H., Iwata, R., Satoh, Y., Ohno, H., Yamada, K., and Iino, Y. (2013).
988 Concentration memory-dependent synaptic plasticity of a taste circuit regulates salt
989 concentration chemotaxis in Caenorhabditis elegans. Nat Commun *4*, 2210.

990 Lackner, M.R., Nurrish, S.J., and Kaplan, J.M. (1999). Facilitation of synaptic transmission by
991 EGL-30 Gqalpha and EGL-8 PLCbeta: DAG binding to UNC-13 is required to stimulate
992 acetylcholine release. Neuron *24*, 335-346.
993 LeBoeuf, B., Chen, X., and Garcia, L.R. (2020). WNT regulates programmed muscle remodeling
994 through PLC-beta and calcineurin in Caenorhabditis elegans males. Development *147*.
995 Li, B., Jie, W., Huang, L., Wei, P., Li, S., Luo, Z., Friedman, A.K., Meredith, A.L., Han, M.H., Zhu,
996 X.H.*, et al.* (2014). Nuclear BK channels regulate gene expression via the control of
997 nuclear calcium signaling. Nat Neurosci *17*, 1055-1063.
998 Li, P., Collins, K.M., Koelle, M.R., and Shen, K. (2013). LIN-12/Notch signaling instructs
999 postsynaptic muscle arm development by regulating UNC-40/DCC and MADD-2 in
1000 Caenorhabditis elegans. Elife *2*, e00378.
1001 Lou, X., Korogod, N., Brose, N., and Schneggenburger, R. (2008). Phorbol esters modulate
1002 spontaneous and Ca2+-evoked transmitter release via acting on both Munc13 and protein
1003 kinase C. J Neurosci *28*, 8257-8267.
1004 Lutz, S., Freichel-Blomquist, A., Yang, Y., Rumenapp, U., Jakobs, K.H., Schmidt, M., and
1005 Wieland, T. (2005). The guanine nucleotide exchange factor p63RhoGEF, a specific link
1006 between Gq/11-coupled receptor signaling and RhoA. J Biol Chem *280*, 11134-11139.
1007 Maruyama, I.N., and Brenner, S. (1991). A phorbol ester/diacylglycerol-binding protein encoded
1008 by the unc-13 gene of Caenorhabditis elegans. Proc Natl Acad Sci U S A *88*, 5729-5733.
1009 McMullan, R., Hiley, E., Morrison, P., and Nurrish, S.J. (2006). Rho is a presynaptic activator of
1010 neurotransmitter release at pre-existing synapses in C. elegans. Genes Dev *20*, 65-76.
1011 McMullan, R., and Nurrish, S.J. (2011). The RHO-1 RhoGTPase modulates fertility and multiple
1012 behaviors in adult C. elegans. PLoS One *6*, e17265.

1013 Mendel, J.E., Korswagen, H.C., Liu, K.S., Hajdu-Cronin, Y.M., Simon, M.I., Plasterk, R.H., and
1014 Sternberg, P.W. (1995). Participation of the protein Go in multiple aspects of behavior in
1015 C. elegans. Science *267*, 1652-1655.
1016 Miller, K.G., Alfonso, A., Nguyen, M., Crowell, J.A., Johnson, C.D., and Rand, J.B. (1996). A
1017 genetic selection for Caenorhabditis elegans synaptic transmission mutants. Proc Natl
1018 Acad Sci U S A *93*, 12593-12598.
1019 Miller, K.G., Emerson, M.D., and Rand, J.B. (1999). Goalpha and diacylglycerol kinase
1020 negatively regulate the Gqalpha pathway in C. elegans. Neuron *24*, 323-333.
1021 Moresco, J.J., and Koelle, M.R. (2004). Activation of EGL-47, a Galpha(o)-coupled receptor,
1022 inhibits function of hermaphrodite-specific motor neurons to regulate Caenorhabditis
1023 elegans egg-laying behavior. J Neurosci *24*, 8522-8530.
1024 Mujica, P.E., and Gonzalez, F.G. (2011). Interaction between IP(3) receptors and BK channels
1025 in arterial smooth muscle: non-canonical IP(3) signaling at work. J Gen Physiol *137*, 473-
1026 477.
1027 Newton, A.C. (2001). Protein kinase C: structural and spatial regulation by phosphorylation,
1028 cofactors, and macromolecular interactions. Chem Rev *101*, 2353-2364.
1029 Nurrish, S., Segalat, L., and Kaplan, J.M. (1999). Serotonin inhibition of synaptic transmission:
1030 Galpha(0) decreases the abundance of UNC-13 at release sites. Neuron *24*, 231-242.
1031 Oakes, M., Law, W.J., and Komuniecki, R. (2019). Cannabinoids Stimulate the TRP Channel-
1032 Dependent Release of Both Serotonin and Dopamine to Modulate Behavior in C. elegans.
1033 J Neurosci *39*, 4142-4152.
1034 Oakes, M.D., Law, W.J., Clark, T., Bamber, B.A., and Komuniecki, R. (2017). Cannabinoids
1035 Activate Monoaminergic Signaling to Modulate Key C. elegans Behaviors. J Neurosci *37*,
1036 2859-2869.

1037 Offermanns, S. (2001). In vivo functions of heterotrimeric G-proteins: studies in Galpha-deficient
1038 mice. Oncogene *20*, 1635-1642.
1039 Ohno, H., Sakai, N., Adachi, T., and Iino, Y. (2017). Dynamics of Presynaptic Diacylglycerol in
1040 a Sensory Neuron Encode Differences between Past and Current Stimulus Intensity. Cell
1041 Rep *20*, 2294-2303.
1042 Okochi, Y., Kimura, K.D., Ohta, A., and Mori, I. (2005). Diverse regulation of sensory signaling
1043 by C. elegans nPKC-epsilon/eta TTX-4. EMBO J *24*, 2127-2137.
1044 Pastuhov, S.I., Matsumoto, K., and Hisamoto, N. (2016). Endocannabinoid signaling regulates
1045 regenerative axon navigation in Caenorhabditis elegans via the GPCRs NPR-19 and NPR-
1046 32. Genes Cells *21*, 696-705.
1047 Pereira, L., Kratsios, P., Serrano-Saiz, E., Sheftel, H., Mayo, A.E., Hall, D.H., White, J.G.,
1048 LeBoeuf, B., Garcia, L.R., Alon, U.*, et al.* (2015). A cellular and regulatory map of the
1049 cholinergic nervous system of C. elegans. Elife *4*.
1050 Porter, M.Y., and Koelle, M.R. (2010). RSBP-1 is a membrane-targeting subunit required by the
1051 Galpha(q)-specific but not the Galpha(o)-specific R7 regulator of G protein signaling in
1052 Caenorhabditis elegans. Mol Biol Cell *21*, 232-243.
1053 Ravi, B., Garcia, J., and Collins, K.M. (2018a). Homeostatic Feedback Modulates the
1054 Development of Two-State Patterned Activity in a Model Serotonin Motor Circuit in
1055 Caenorhabditis elegans. J Neurosci *38*, 6283-6298.
1056 Ravi, B., Nassar, L.M., Kopchock, R.J., 3rd, Dhakal, P., Scheetz, M., and Collins, K.M. (2018b).
1057 Ratiometric Calcium Imaging of Individual Neurons in Behaving Caenorhabditis Elegans.
1058 J Vis Exp.
1059 Ravi, B., Zhao, J., Chaudhry, I., Signorelli, R., Bartole, M., Kopchock, R.J., Guijarro, C., Kaplan,
1060 J.M., Kang, L., and Collins, K.M. (2021). Presynaptic Galphao (GOA-1) signals to depress

1061 command neuron excitability and allow stretch-dependent modulation of egg laying in
1062 Caenorhabditis elegans. Genetics.
1063 Reiner, D.J., Newton, E.M., Tian, H., and Thomas, J.H. (1999). Diverse behavioural defects
1064 caused by mutations in Caenorhabditis elegans unc-43 CaM kinase II. Nature *402*, 199-
1065 203.
1066 Reiner, D.J., Weinshenker, D., Tian, H., Thomas, J.H., Nishiwaki, K., Miwa, J., Gruninger, T.,
1067 Leboeuf, B., and Garcia, L.R. (2006). Behavioral genetics of caenorhabditis elegans unc-
1068 103-encoded erg-like K(+) channel. J Neurogenet *20*, 41-66.
1069 Reynolds, N.K., Schade, M.A., and Miller, K.G. (2005). Convergent, RIC-8-dependent Galpha
1070 signaling pathways in the Caenorhabditis elegans synaptic signaling network. Genetics
1071 *169*, 651-670.
1072 Rojas, R.J., Yohe, M.E., Gershburg, S., Kawano, T., Kozasa, T., and Sondek, J. (2007). Galphaq
1073 directly activates p63RhoGEF and Trio via a conserved extension of the Dbl homology-
1074 associated pleckstrin homology domain. J Biol Chem *282*, 29201-29210.
1075 Rose, A.M., and Baillie, D.L. (1980). Genetic organization of the region around UNC-15 (I), a
1076 gene affecting paramyosin in Caenorhabditis elegans. Genetics *96*, 639-648.
1077 Rozengurt, E., Sinnett-Smith, J., and Zugaza, J.L. (1997). Protein kinase D: a novel target for
1078 diacylglycerol and phorbol esters. Biochem Soc Trans *25*, 565-571.
1079 Seifert, J.P., Zhou, Y., Hicks, S.N., Sondek, J., and Harden, T.K. (2008). Dual activation of
1080 phospholipase C-epsilon by Rho and Ras GTPases. J Biol Chem *283*, 29690-29698.
1081 Shimizu, T., Pastuhov, S.I., Hanafusa, H., Matsumoto, K., and Hisamoto, N. (2018). The
1082 C. elegans BRCA2-ALP/Enigma Complex Regulates Axon Regeneration via a Rho
1083 GTPase-ROCK-MLC Phosphorylation Pathway. Cell Rep *24*, 1880-1889.
1084 Shyn, S.I., Kerr, R., and Schafer, W.R. (2003). Serotonin and Go modulate functional states of
1085 neurons and muscles controlling C. elegans egg-laying behavior. Curr Biol *13*, 1910-1915.

1086 Sieburth, D., Madison, J.M., and Kaplan, J.M. (2007). PKC-1 regulates secretion of
1087 neuropeptides. Nat Neurosci *10*, 49-57.
1088 Silinsky, E.M., and Searl, T.J. (2003). Phorbol esters and neurotransmitter release: more than
1089 just protein kinase C? Br J Pharmacol *138*, 1191-1201.
1090 Simon, M.I., Strathmann, M.P., and Gautam, N. (1991). Diversity of G proteins in signal
1091 transduction. Science *252*, 802-808.
1092 Soltesz, I., Alger, B.E., Kano, M., Lee, S.H., Lovinger, D.M., Ohno-Shosaku, T., and Watanabe,
1093 M. (2015). Weeding out bad waves: towards selective cannabinoid circuit control in
1094 epilepsy. Nat Rev Neurosci *16*, 264-277.
1095 Stauffer, T.P., Ahn, S., and Meyer, T. (1998). Receptor-induced transient reduction in plasma
1096 membrane PtdIns(4,5)P2 concentration monitored in living cells. Curr Biol *8*, 343-346.
1097 Steven, R., Kubiseski, T.J., Zheng, H., Kulkarni, S., Mancillas, J., Ruiz Morales, A., Hogue, C.W.,
1098 Pawson, T., and Culotti, J. (1998). UNC-73 activates the Rac GTPase and is required for
1099 cell and growth cone migrations in C. elegans. Cell *92*, 785-795.
1100 Steven, R., Zhang, L., Culotti, J., and Pawson, T. (2005). The UNC-73/Trio RhoGEF-2 domain
1101 is required in separate isoforms for the regulation of pharynx pumping and normal
1102 neurotransmission in C. elegans. Genes Dev *19*, 2016-2029.
1103 Suh, B.C., Inoue, T., Meyer, T., and Hille, B. (2006). Rapid chemically induced changes of
1104 PtdIns(4,5)P2 gate KCNQ ion channels. Science *314*, 1454-1457.
1105 Tabuse, Y. (2002). Protein kinase C isotypes in C. elegans. J Biochem *132*, 519-522.
1106 Tabuse, Y., and Miwa, J. (1983). A gene involved in action of tumor promoters is identified and
1107 mapped in Caenorhabditis elegans. Carcinogenesis *4*, 783-786.
1108 Tabuse, Y., Nishiwaki, K., and Miwa, J. (1989). Mutations in a protein kinase C homolog confer
1109 phorbol ester resistance on Caenorhabditis elegans. Science *243*, 1713-1716.

1110 Tanimura, A., Yamazaki, M., Hashimotodani, Y., Uchigashima, M., Kawata, S., Abe, M., Kita, Y.,
1111 Hashimoto, K., Shimizu, T., Watanabe, M.*, et al.* (2010). The endocannabinoid 2-
1112 arachidonoylglycerol produced by diacylglycerol lipase alpha mediates retrograde
1113 suppression of synaptic transmission. Neuron *65*, 320-327.
1114 Tanis, J.E., Moresco, J.J., Lindquist, R.A., and Koelle, M.R. (2008). Regulation of serotonin
1115 biosynthesis by the G proteins Galphao and Galphaq controls serotonin signaling in
1116 Caenorhabditis elegans. Genetics *178*, 157-169.
1117 Taylor, S.R., Santpere, G., Weinreb, A., Barrett, A., Reilly, M.B., Xu, C., Varol, E., Oikonomou,
1118 P., Glenwinkel, L., McWhirter, R.*, et al.* (2021). Molecular topography of an entire nervous
1119 system. Cell *184*, 4329-4347 e4323.
1120 Tewson, P., Westenberg, M., Zhao, Y., Campbell, R.E., Quinn, A.M., and Hughes, T.E. (2012).
1121 Simultaneous detection of Ca2+ and diacylglycerol signaling in living cells. PLoS One *7*,
1122 e42791.
1123 Thomas, J.H. (1990). Genetic analysis of defecation in Caenorhabditis elegans. Genetics *124*,
1124 855-872.
1125 Thore, S., Dyachok, O., Gylfe, E., and Tengholm, A. (2005). Feedback activation of
1126 phospholipase C via intracellular mobilization and store-operated influx of Ca2+ in insulin-
1127 secreting beta-cells. J Cell Sci *118*, 4463-4471.
1128 Trent, C., Tsuing, N., and Horvitz, H.R. (1983). Egg-laying defective mutants of the nematode
1129 Caenorhabditis elegans. Genetics *104*, 619-647.
1130 Vázquez-Manrique, R.P., Nagy, A.I., Legg, J.C., Bales, O.A., Ly, S., and Baylis, H.A. (2008).
1131 Phospholipase C-epsilon regulates epidermal morphogenesis in Caenorhabditis elegans.
1132 PLoS Genet *4*, e1000043.
1133 Ventimiglia, D., and Bargmann, C.I. (2017). Diverse modes of synaptic signaling, regulation, and
1134 plasticity distinguish two classes of C. elegans glutamatergic neurons. Elife *6*.

1135 Waggoner, L.E., Dickinson, K.A., Poole, D.S., Tabuse, Y., Miwa, J., and Schafer, W.R. (2000).
1136 Long-term nicotine adaptation in Caenorhabditis elegans involves PKC-dependent
1137 changes in nicotinic receptor abundance. J Neurosci *20*, 8802-8811.
1138 Waggoner, L.E., Zhou, G.T., Schafer, R.W., and Schafer, W.R. (1998). Control of alternative
1139 behavioral states by serotonin in Caenorhabditis elegans. Neuron *21*, 203-214.
1140 Wei, A.D., Butler, A., and Salkoff, L. (2005). KCNQ-like potassium channels in Caenorhabditis
1141 elegans. Conserved properties and modulation. J Biol Chem *280*, 21337-21345.
1142 Weinshenker, D., Wei, A., Salkoff, L., and Thomas, J.H. (1999). Block of an ether-a-go-go-like
1143 K(+) channel by imipramine rescues egl-2 excitation defects in Caenorhabditis elegans. J
1144 Neurosci *19*, 9831-9840.
1145 Wettschureck, N., van der Stelt, M., Tsubokawa, H., Krestel, H., Moers, A., Petrosino, S., Schütz,
1146 G., Di Marzo, V., and Offermanns, S. (2006). Forebrain-specific inactivation of Gq/G11
1147 family G proteins results in age-dependent epilepsy and impaired endocannabinoid
1148 formation. Mol Cell Biol *26*, 5888-5894.
1149 White, J.G., Southgate, E., Thomson, J.N., and Brenner, S. (1986). The structure of the nervous
1150 system of the nematode Caenorhabditis elegans. Philos Trans R Soc Lond B Biol Sci *314*,
1151 1-340.
1152 Wilke, B.U., Lindner, M., Greifenberg, L., Albus, A., Kronimus, Y., Bunemann, M., Leitner, M.G.,
1153 and Oliver, D. (2014). Diacylglycerol mediates regulation of TASK potassium channels by
1154 Gq-coupled receptors. Nat Commun *5*, 5540.
1155 Wilkie, T.M., Gilbert, D.J., Olsen, A.S., Chen, X.N., Amatruda, T.T., Korenberg, J.R., Trask, B.J.,
1156 de Jong, P., Reed, R.R., Simon, M.I.*, et al.* (1992). Evolution of the mammalian G protein
1157 alpha subunit multigene family. Nat Genet *1*, 85-91.

1158 Williams, S.L., Lutz, S., Charlie, N.K., Vettel, C., Ailion, M., Coco, C., Tesmer, J.J., Jorgensen,
1159 E.M., Wieland, T., and Miller, K.G. (2007). Trio's Rho-specific GEF domain is the missing
1160 Galpha q effector in C. elegans. Genes Dev *21*, 2731-2746.
1161 Wing, M.R., Snyder, J.T., Sondek, J., and Harden, T.K. (2003). Direct activation of
1162 phospholipase C-epsilon by Rho. J Biol Chem *278*, 41253-41258.
1163 Xiao, H., Hapiak, V.M., Smith, K.A., Lin, L., Hobson, R.J., Plenefisch, J., and Komuniecki, R.
1164 (2006). SER-1, a Caenorhabditis elegans 5-HT2-like receptor, and a multi-PDZ domain
1165 containing protein (MPZ-1) interact in vulval muscle to facilitate serotonin-stimulated egg-
1166 laying. Dev Biol *298*, 379-391.
1167 Xiao, L., Eto, M., and Kazanietz, M.G. (2009). ROCK mediates phorbol ester-induced apoptosis
1168 in prostate cancer cells via p21Cip1 up-regulation and JNK. J Biol Chem *284*, 29365-
1169 29375.
1170 Yang, L., Dai, F., Tang, L., Le, Y., and Yao, W. (2017). Macrophage differentiation induced by
1171 PMA is mediated by activation of RhoA/ROCK signaling. J Toxicol Sci *42*, 763-771.
1172 Yin, X., Gower, N.J., Baylis, H.A., and Strange, K. (2004). Inositol 1,4,5-trisphosphate signaling
1173 regulates rhythmic contractile activity of myoepithelial sheath cells in Caenorhabditis
1174 elegans. Mol Biol Cell *15*, 3938-3949.
1175 Yook, K., and Hodgkin, J. (2007). Mos1 mutagenesis reveals a diversity of mechanisms affecting
1176 response of Caenorhabditis elegans to the bacterial pathogen Microbacterium
1177 nematophilum. Genetics *175*, 681-697.
1178 Yu, H., Aleman-Meza, B., Gharib, S., Labocha, M.K., Cronin, C.J., Sternberg, P.W., and Zhong,
1179 W. (2013). Systematic profiling of Caenorhabditis elegans locomotive behaviors reveals
1180 additional components in G-protein Galphaq signaling. Proc Natl Acad Sci U S A *110*,
1181 11940-11945.

1182 Zhang, M., Chung, S.H., Fang-Yen, C., Craig, C., Kerr, R.A., Suzuki, H., Samuel, A.D., Mazur,
1183 E., and Schafer, W.R. (2008). A self-regulating feed-forward circuit controlling C. elegans
1184 egg-laying behavior. Curr Biol *18*, 1445-1455.
1185 Zhang, M., Schafer, W.R., and Breitling, R. (2010). A circuit model of the temporal pattern
1186 generator of Caenorhabditis egg-laying behavior. BMC Syst Biol *4*, 81.
1187